Quantum State Smoothing Cannot Be Assumed Classical Even When the Filtering and Retrofiltering Are Classical

Kiarn T. Laverick,[1,*] Prahlad Warszawski,[2] Areeya Chantasri,[1,3] and Howard M. Wiseman[1,4,†]

[1] *Centre for Quantum Computation and Communication Technology (Australian Research Council), Centre for Quantum Dynamics, Griffith University, Yuggera Country, Brisbane, Queensland 4111, Australia*

[2] *Centre of Excellence in Engineered Quantum Systems (Australian Research Council), School of Physics, The University of Sydney, Gadigal Country, Sydney, New South Wales 2006, Australia*

[3] *Optical and Quantum Physics Laboratory, Department of Physics, Faculty of Science, Mahidol University, Bangkok, 10140, Thailand*

[4] *Institute for Quantum Studies, Chapman University, Orange, California 92866, USA*

(Received 23 May 2023; accepted 8 November 2023; published 11 December 2023)

State smoothing is a technique to estimate a state at a particular time, conditioned on information obtained both before (past) and after (future) that time. For a classical system, the smoothed state is a normalized product of the *filtered state* (a state conditioned only on the past measurement information and the initial preparation) and the *retrofiltered effect* (depending only on the future measurement information). For the quantum case, while there are well-established analogues of the filtered state (ρ_F) and the retrofiltered effect ($\hat{E}_R$), their product does not, in general, provide a valid quantum state for smoothing. However, this procedure does seem to work when ρ_F and $\hat{E}_R$ are mutually diagonalizable. This fact has been used to obtain smoothed quantum states—purer than the filtered states—in a number of experiments on continuously monitored quantum systems, in cavity QED and atomic systems. In this paper we show that there is an implicit assumption underlying this technique: that if all the information were known to the observer, the true system state would be one of the diagonal basis states. This assumption does not necessarily hold, as the missing information is quantum information. It could be known to the observer only if it were turned into a classical measurement record, but then its nature would depend on the choice of measurement. We show by a simple model that, depending on that measurement choice, the smoothed quantum state can: agree with that from the classical method, disagree with it but still be co-diagonal with it, or not even be co-diagonal with it. That is, just because filtering and retrofiltering appear classical does not mean classical smoothing theory is applicable in quantum experiments.

DOI: 10.1103/PRXQuantum.4.040340

I. MOTIVATION AND SYNOPSIS

Imagine a two-level atom whose dynamics comprise incoherent excitations and de-excitations, the latter by radiative damping. Say you are monitoring some fraction of the atom's radiation and, after some time, you see a photon. What do you think the state of the atom was immediately before this photon was emitted? (See Fig. 1.)

If you answered "the excited state," then you probably have intuition grounded in classical smoothing theory, as will be shown. Smoothing is a technique an observer can use to estimate the true state $\mathbf{x}_T$ of a stochastically evolving system, using information $\mathbf{O}$ the observer obtains from continuously monitoring the system. The true state is typically not known exactly because there is other information, $\mathbf{U}$, that is unknown to the observer. As such, the most general form of the state of the system is a probability distribution $\wp(\mathbf{x};t)$ for the event $\mathbf{x}=\mathbf{x}_T$. One technique for estimating the state at time t is filtering, in which $\wp(\mathbf{x};t)$ is conditioned on the record $\overleftarrow{\mathbf{O}}_t$ before t. Another is *retrofiltering*, which uses the record $\overrightarrow{\mathbf{O}}_t$ after t. However, the best estimate comes from *smoothing*, which is conditioning on the entire record, $\overleftrightarrow{\mathbf{O}}$. The smoothed distribution is simply related to the previous two techniques:

$$\wp_S(\mathbf{x};t)=\wp(\mathbf{x};t|\overleftrightarrow{\mathbf{O}})\propto E_R(\mathbf{x};t)\wp_F(\mathbf{x};t). \tag{1}$$

Here $\wp_F(\mathbf{x};t):=\wp(\mathbf{x};t|\overleftarrow{\mathbf{O}}_t)$ is called the "filtered state"

*dr.kiarn.laverick@gmail.com

†prof.howard.wiseman@gmail.com

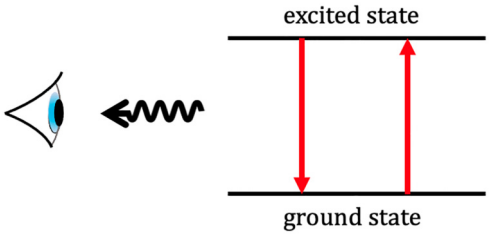

FIG. 1. An incoherently excited and damped two-level atom that has emitted a photon that is subsequently observed. What was the state of the atom a short time before the photon was emitted (as inferred from its detection time)?

and $E_R(\mathbf{x};t) \propto \wp(\overrightarrow{\mathbf{O}}_t|\mathbf{x},t)$ is the retrofiltered effect.

In quantum state estimation, there are well-established analogues: the filtered state $\rho_F(t)$ and the retrofiltered effect [positive operator-valued measure (POVM) element] $\hat{E}_R(t)$, where we borrowed the term "effect" in the classical case for consistency. However, quantum smoothing is not so straightforward.

If ρ_F is not pure, this implies that there is information missing to the observer. Thus, intuitively, it should be possible to obtain a better estimate by smoothing, by using $\overleftrightarrow{\mathbf{O}}$ instead of just $\overleftarrow{\mathbf{O}}_t$. Naively following the classical form (1) and multiplying $\rho_F(t)$ and $\hat{E}_R(t)$ does not, in general, lead to a valid quantum state [1]. However, there is one case where it does: when $\rho_F(t)$ and $\hat{E}_R(t)$ are co-diagonal in some basis. Then multiplying these quantities replicates exactly the classical smoothing calculation (1), with the diagonal elements in these matrices acting like classical probabilities for the true state.

The applicability of classical smoothing theory for quantum systems where both the filtering and the retrofiltering have this classical description seems quite reasonable. It has been used in a number of experiments on quantum systems where the diagonal states are dressed atom-field states [2,3], atomic energy levels [4], and photon number states [5]. It also seems obviously applicable to the scenario introduced in the first paragraph, and Fig. 1, with the diagonal basis states being the atomic excited and ground states. But can it really be justified?

In this paper we show that classical smoothing gives the best estimate for the true quantum state only with an extra assumption: that the missing information is such that, if it were known, the state would be in one of the diagonal basis states. While this assumption may seem plausible, it is not entailed by the dynamics. If the system is quantum, then the missing information is also quantum. For it to be knowable, in principle, it must be turned into a classical measurement record, a secondary record $\mathbf{U}$ alongside the primary observer's record $\mathbf{O}$. Then the smoothed quantum state [1], denoted ρ_S, can be defined as the optimal estimate [6,7] of the state conditioned on both $\overleftarrow{\mathbf{O}}$ and $\overleftarrow{\mathbf{U}}$ (i.e., the true state, denoted ρ_T) by the observer who knows $\overleftrightarrow{\mathbf{O}}$ but not $\overleftarrow{\mathbf{U}}$. Crucially, the nature of the unknown measurement record, $\overleftarrow{\mathbf{U}}$, depends on the type of detector that creates the corresponding record from the missing quantum information in the system's environment.

We consider three different ways to perform the secondary measurement, to prove various results relevant to our argument. In all cases, we use the same simple system, and the primary observer performs the same type of measurement, for which ρ_F and $\hat{E}_R$ are co-diagonal. Indeed, the system and its dynamics, as well as the primary measurement and its result, exactly correspond to those in Fig. 1. For the first choice of secondary measurement, the true state ρ_T is a pure state in the co-diagonal basis of ρ_F and $\hat{E}_R$, and ρ_S reproduces the classical smoothed state, as expected. For the second choice, ρ_T is not in this diagonal basis, and a different ρ_S is obtained, albeit one that is still diagonal in this basis. For the third choice, ρ_T is again not in this diagonal basis, but this time the smoothed state ρ_S is also not co-diagonal with the classically obtained smoothed state. We further show that, contrary to what one might expect, the classically obtained smoothed state is not even the most optimal in terms of the expected value of the cost function that defines the smoothed quantum state. Our results highlight and delineate the limitations of applying classical estimation techniques to quantum systems even when they seem adequate.

II. OUTLINE

In Sec. III, we review classical state smoothing in the classical setting as well as how it has been applied to quantum systems. We then discuss some actual experimental examples that have used classical smoothing theory before we introduce quantum state smoothing theory. In Sec. IV, we summarize the three main results of this paper and provide a rough outline of the arguments that lead to them.

In Sec. V, we introduce the physical system that will serve to prove our results. In Sec. V A, we specify the type of measurement (by Alice, say) on the system outputs that will yield the observed records on which all of the state estimates are conditioned. Alice's measurements are chosen such that the filtered state and the retrofiltered effect are co-diagonal, the situation in which classical smoothing theory would seem appropriate. In Sec. V B, we consider the system outputs that are not accessible to Alice. We specify a measurement (by Bob, say) on these system outputs such that the optimal estimate by Alice, using quantum state smoothing [6,7], coincides with the optimal estimate obtained by classical smoothing. Before moving on, we compare this smoothed quantum state with the filtered state to attain a deeper understanding of the physical system in this regime. We also resolve what may seem a puzzling feature of the expected cost functions that define

these optimal states so as to lay the groundwork for later results on this subject in this paper. The subsequent three sections are dedicated to our proving its three main results. In Sec. VI, by changing Bob's measurement scheme to a homodyne measurement, we show that the smoothed quantum state does not necessarily reduce to the classically smoothed state independent of the choice of secondary measurement (Result 1). In Sec. VII, we again change Bob's measurement strategy, this time to an adaptive measurement scheme, to show that the smoothed quantum state is not even necessarily co-diagonal with the filtered state and retrofiltered effect (Result 2). In Sec. VIII, we compare which of these three cases yields the lowest expected cost function, and hence could be the most desirable choice of assumed measurement for Bob, showing that for most of the time the classical case performs the worst (Result 3). Lastly, in Sec. IX, we conclude the paper, and provide some questions for future research.

III. CLASSICAL AND QUANTUM STATE SMOOTHING

A. Classical state smoothing

For ease of presentation, we consider classical systems that can be described by a countable number of discrete-valued parameters, collected in a vector $\mathbf{x} \in \mathbb{X}$, called the "configuration." The characteristic of classical systems is that there exists a true or objective configuration $\mathbf{x}_T(t)$, defining definite values for these parameters. It is only through one's lack of knowledge of the initial configuration of the system and the environment with which it interacts that this value is obscured. Therefore, the best description one can give of the parameters is through the state $\wp(\mathbf{x};t)$, a non-negative distribution over possible true configurations normalized such that $\sum_{\mathbf{x}\in\mathbb{X}} \wp(\mathbf{x};t) = 1$. This state, in general, has nonzero entropy; to use quantum terminology, it is a mixed state, unlike the pure state $\wp_T(\mathbf{x};t) = \delta_{\mathbf{x},\mathbf{x}_T(t)}$ corresponding to the true configuration.

Often, the mixedness of a state will increase over time due to interaction with the environment. However, through measurement, which we take to be a continuous-in-time measurement, one can gain information about the hidden true state. Note that since we are considering only discrete classical systems, the dynamics of the configuration are restricted to transitions between the points in $\mathbb{X}$. We further restrict ourselves to Markovian systems; that is, both the measurement results at time t and the state of the system at time $t + dt$ are governed only by the state at the current time, without the need to specify any of the states before that. This model of classical systems is commonly referred to as a "hidden Markov model," as the true state underlying the observed measurement results is hidden.

Given information about the system, in the form of a measurement record $\mathbf{O}$, one can ask: what is the best estimate $\check{\wp}(\mathbf{x};t)$ of the true state using that information? Here we use a check (rather than the more common hat) to denote an estimate so as to prevent confusion with quantum operators, for which we will use hats. To define this optimal estimate, one needs a measure of closeness between the estimated state and the true state; we choose the sum-square deviation cost function,

$$\mathcal{C}[\check{\wp}, \wp_T] = \sum_{\mathbf{x}\in\mathbb{X}} [\check{\wp}(\mathbf{x};t) - \wp_T(\mathbf{x};t)]^2. \tag{2}$$

This cost function is the state analogue of the square error cost function that is often used when one is directly estimating the configuration instead of the state.

The cost function given above depends on the true state, which is, of course, unknown since it is what one is trying to estimate. Thus, one must consider a way to turn the cost function into a value (to be minimized) that is independent of the true state. The simplest way is the Bayesian approach to estimation [8–11], in which one aims to minimize an *expected* cost function given the available measurement record, defined as

$$\mathcal{B}_C[\check{\wp}] = \mathbb{E}_{\wp_T|\mathbf{O}_C}\{\mathcal{C}[\check{\wp}, \wp_T]\}, \tag{3}$$

where $\mathbb{E}_{X|Y}\{Z\}$ denotes an ensemble average of Z over X given Y, where as a convention X is omitted when $X = Z$. We have introduced a dummy subscript "C" (standing for conditioning) on $\mathbf{O}$ to denote what part of the measurement record is available. For example, one has a filtered conditioning $C = F$ if only the past measurement record, i.e., $\mathbf{O}_F = \overleftarrow{\mathbf{O}}_t = \{\mathbf{y}(\tau) : \tau \in [t_i, t)\}$, is available. Here $\mathbf{y}(\tau)$ is the measurement outcome (detector click, photocurrent, etc.) at time τ and t_i is the initial time. Similarly, to have a smoothed conditioning $C = S$, we must have access to the past-future measurement record $\mathbf{O}_S = \overleftrightarrow{\mathbf{O}} = \{\mathbf{y}(\tau) : \tau \in [t_i, t_f)\}$, where t_f is the final time.

It is easy to show, by one setting to zero the derivative of Eq. (3) with respect to $\check{\wp}$ and solving for $\check{\wp}$ [7], that the optimal estimator for this sum-square deviation cost function is given by

$$\wp_C^{\text{opt}}(\mathbf{x};t) = \mathbb{E}_{|\mathbf{O}_C}\{\wp_T(\mathbf{x};t)\}. \tag{4}$$

By substituting the true state $\wp_T(\mathbf{x};t) = \delta_{\mathbf{x},\mathbf{x}_T(t)}$, we can simplify the computation of Eq. (4) drastically, obtaining $\wp_C^{\text{opt}}(\mathbf{x};t) = \wp(\mathbf{x};t|\mathbf{O}_C)$. Thus, the optimal filtered estimate of the true state is defined as

$$\wp_F^{\text{opt}}(\mathbf{x};t) = \wp(\mathbf{x};t|\overleftarrow{\mathbf{O}}_t). \tag{5}$$

Similarly, the optimal smoothed estimate is defined as

$$\wp_S^{\text{opt}}(\mathbf{x};t) = \wp(\mathbf{x};t|\overleftrightarrow{\mathbf{O}}) \propto E_R(\mathbf{x};t)\,\wp_F(\mathbf{x};t), \tag{6}$$

where

$$E_R(\mathbf{x};t) = \wp(\overrightarrow{\mathbf{O}}_t|\mathbf{x},t) \tag{7}$$

is also a non-negative function over possible configurations. Borrowing terminology from quantum measurement theory, we call $E_R(\mathbf{x};t)$ an effect. Specifically, because it involves the measurement record over the whole future, we call it a "retrofiltered (R) effect." Equation (6) can be derived by applying Bayes' theorem and remembering that the system is Markovian. Thus, the optimal smoothed state involves both the optimal filtering and the Bayesian retrofiltering.

B. Quantizing state estimation

In open quantum systems an idea similar to classical state estimation exists, where one instead aims to give an estimated quantum state, $\rho(t)$, based on the outcomes of a continuous-in-time measurement. The ideas of both filtering and retrofiltering translate quite naturally to quantum systems. Quantum filtering [12,13], also known as quantum trajectory theory [14,15], is concerned with determining the conditional evolution of the quantum state of an open quantum system where the environment is subjected to a continuous-in-time measurement. This conditional state is called the "filtered quantum state" $\rho_F(t) := \rho_{\overleftarrow{\mathbf{O}}_t}$, the analogue of $\wp_F(\mathbf{x};t)$, as it conditions the state of the system on all measurement outcomes up until the estimation time t. This analogy is actually very close; the dynamical map in quantum trajectory theory is an obvious quantization of the dynamical map in classical filtering [15].

For retrofiltering, the likelihood function $\wp(\overrightarrow{\mathbf{O}}_t|\mathbf{x},t)$ is replaced by a quantum effect, i.e., a POVM element. In quantum measurement theory [15–17], a POVM is a set of positive Hermitian operators $\{\hat{E}_o\}$ whose elements have an expectation value equal to the probability of outcome o occurring, i.e., $\mathrm{Tr}[\hat{E}_o\rho] = \wp(o|\rho)$. From this, it is easy to see that the quantum analogue of the classical retrofiltered effect is the operator $\hat{E}_R(t)$ defined such that $\wp(\overrightarrow{\mathbf{O}}_t|\rho,t) = \mathrm{Tr}[\hat{E}_R(t)\rho]$.

With both filtering and retrofiltering having a direct quantum analogue, one would be forgiven for assuming that the smoothing technique also has some trivial quantization. Based on the classical formula for smoothing in Eq. (6), one might define the smoothed quantum state as [18,19]

$$\varrho_{\mathrm{SWV}}(t) = \frac{\hat{E}_R(t) \circ \rho_F(t)}{\mathrm{Tr}[\hat{E}_R(t) \circ \rho_F(t)]}, \tag{8}$$

where the Jordan product, defined as $A \circ B = \frac{1}{2}(AB + BA)$, is used to ensure that the operator is Hermitian, and the denominator is for normalization. The subscript "SWV" will be made clear shortly. However, because the filtered state and the retrofiltered effect do not commute, in general, this construction does not always yield a valid (i.e., positive semidefinite) quantum state. Therefore, one cannot use it as the general definition of the smoothed quantum state. This operator has a close connection to weak values (see Ref. [7] for an in-depth discussion), and we refer to ρ_{SWV}, following Refs. [7,20], as the "smoothed weak-value (SWV) state."

C. Quantum experiments involving smoothing of the state

While the naive quantization [Eq. 8] of the smoothed quantum state does not generally yield a valid estimate, state smoothing has been applied with apparent success in several quantum experiments. All of them were done in cavity QED, a platform known for high-efficiency continuous measurements and superb control of individual quantum systems [21]. They all succeeded in obtaining a valid quantum state when *classical* smoothing techniques were applied to the quantum system. Here we summarize these experiments. Note that it is not essential for the reader to understand the details of the particular experiments to grasp the key results of this paper. The first experiment is that reported in Refs. [2,3]. This experiment involves dropping cesium atoms through a driven optical cavity containing a small number of photons (10–100). Its aim was to experimentally witness the bistability [22] of the dressed atom-field state; that is, the tendency of the joint state of a single atom and field, in the strong-coupling limit, to rapidly relax to two very nearly orthogonal states, switching between them as in a so-called random telegraph signal [23,24]. To demonstrate this phenomenon, the study authors estimated the phase quadrature of the intracavity field using the measurement record arising from homodyne detection of the cavity output beam. To obtain the best estimate, the study authors used the entire (past-future) record. Specifically, inspired by Ref. [22], they applied classical smoothing to a simplified hidden Markov model with three states, each corresponding to a different conditional expectation value of the phase quadrature of the intracavity field. The positive and negative values correspond to the two different dressed states of the atom and the field, while the state with a zero value for the phase quadrature corresponded to the case (not considered in Ref. [22]) where no atom was present in the cavity. Another simplification they made was not to calculate the full classical smoothed state in Eq. (6). Instead, they plotted just the most likely of the three states given the past-future record.

In the second experiment we consider, reported in Ref. [4], a single cesium atom was trapped within an optical high-finesse cavity in the strong-coupling regime. The aim of the experiment was to estimate the occupation probabilities of two possible energy eigenstates of the cesium atom

as well as to estimate the transition rates between these states. Similarly to the previous experiment, they applied classical state smoothing, where the hidden Markov model assumed in this case comprises the two possible energy eigenstates and a third state introduced to help model the additional energy levels of the atom. To obtain this estimate, they probed the cavity with an on-resonant (with the empty cavity) weak laser, contributing a small number of photons (fewer than one photon on average). The output beam was measured by a single-photon detector, with the sequence of detection times forming the measurement record. The study authors processed this measurement record using classical state smoothing, Eq. (6), to obtain estimates of the occupation probabilities of the energy eigenstates.

The final experiment, reported in Ref. [5], also involves a high-finesse cavity and atoms, but the relevant cavity mode is at microwave frequency, and the focus of attention is on the dynamics of its state. The atoms, which are rubidium atoms in circular Rydberg states, are used just to probe the number of photons in the cavity. Specifically, the Rydberg atom is prepared in a superposition of circular Rydberg eigenstates $|+\rangle = (|50\rangle + |51\rangle)/\sqrt{2}$, where $|50\rangle$ ($|51\rangle$) is a circular state with principal quantum number 50 (51), through interaction with a separate low-finesse microwave cavity. These atoms then interact with the intracavity field, causing a photon-number-dependent relative phase shift ϕ between $|50\rangle$ and $|51\rangle$. As the atom exits the cavity, it interacts with a second low-finesse cavity, which rotates the atomic superposition with some particular relative phase ϕ' to $|50\rangle$ (and the orthogonal state to $|51\rangle$), after which the atomic state is measured projectively. By continuously (at least to a good approximation) probing the system with Rydberg atoms, one forms the measurement record from the outcomes of the projective measurement. However, because of the periodicity of the relative phase shift, this measurement can detect the photon number only modulo k, where for this experiment $k = 8$. The study authors used this measurement record to estimate the photon number probabilities via the classical smoothing theory in Eq. (6), and showed an improvement (higher purity) relative to the estimate obtained with classical filtering theory, Eq. (5). Their hidden Markov model is equivalent to assuming that the intracavity field is in some Fock state $|n\rangle$.

D. Why does classical smoothing seem to work in these experiments?

In all of the experiments described in the previous subsection, the study authors applied classical smoothing theory to systems that are, undoubtedly, quantum, while still obtaining sensible results. Although in none of the papers was the estimate explicitly written down as a quantum state, there is a trivial relationship between the smoothed estimates of the probabilities, $\wp_S(x;t)$, and the corresponding estimate of the state: $\breve{\rho}(t) = \sum_x \wp_S(x;t)|\psi_x\rangle\langle\psi_x|$. Here the set of pure states $\{|\psi_x\rangle\}$ are those assumed in the respective hidden Markov models: dressed atom-field states [2,3], atomic energy states [4], and Fock states [5]. We now examine in detail what makes classical smoothing applicable in these cases.

In all these experiments the quantum states corresponding to the d discrete states in the hidden Markov model are *orthogonal*, or very nearly so. This means that in the orthonormal basis $\{|\psi_x\rangle : \langle\psi_x|\psi_{x'}\rangle = \delta_{x,x'}\}_{x=1}^d$, the "true" quantum state of the system at any given time is given by

$$\rho_T(t) = \sum_{x=1}^{d} \wp_T(x;t)|\psi_x\rangle\langle\psi_x|, \tag{9}$$

with $\wp_T(x;t) = \delta_{x,x_T(t)}$. The important point is that the true state will always be diagonal in this basis, which means that so will the filtered state and the retrofiltered effect (see Appendix A for the proofs). That is,

$$\rho_F(t) = \sum_{x=1}^{d} \wp(x;t|\overleftarrow{\mathbf{O}}_t)|\psi_x\rangle\langle\psi_x|, \tag{10a}$$

$$\hat{E}_R(t) = \sum_{x=1}^{d} \wp(\overrightarrow{\mathbf{O}}_t|x,t)|\psi_x\rangle\langle\psi_x|, \tag{10b}$$

which trivially commute, $[\rho_F(t), \hat{E}_R(t)] = 0$. Since the problem of the smoothed weak-valued state becoming indefinite occurs only when $[\rho_F(t), \hat{E}_R(t)] \neq 0$, the orthogonality assumption removes any possibility of $\varrho_{\mathrm{SWV}}(t)$ becoming physically invalid at any point in the evolution. In this case, the SWV state becomes

$$\rho_S^{\mathrm{cl}}(t) = \sum_{x=1}^{d} \wp_S(x;t)|\psi_x\rangle\langle\psi_x|, \tag{11}$$

where $\wp_S(x;t)$ is defined in Eq. (6). From this point forward, we refer to this as the "classical regime," hence the superscript "cl."

While the assumption [Eqs. (10) and (11)] facilitates the use of the SWV state as a smoothed estimate of the quantum state, it has also effectively removed the "quantumness" from the system as it assumes that all the information that was missed by the observer was classical in nature. Moreover, there is an obvious tension in this semiclassical treatment. On the one hand, a portion of the information in the environment is treated as quantum information, i.e., that portion captured by the observer, whose choice of measurement affects how it is converted into classical information. On the other hand, the remaining portion left in the environment is treated as purely classical, revealing which of the orthogonal basis states the system is in. To

obtain a more consistent treatment of quantum systems, all the information in the environment should be treated on the same footing, being subject to different measurement choices ("unravelings"). But to deal with this generalization requires the quantum state smoothing theory of Ref. [1].

E. Quantum state smoothing

The theory of quantum state smoothing, introduced by Guevara and Wiseman [1] in 2015, had two inspirations in the prior literature. The first was the application of classical smoothing theory to quantum systems as mentioned above, in particular that in the laboratory of Mabuchi [2,3]. The second was the application of smoothing theory to quantum estimation by Tsang [18,25] in 2009. Because of the improvements that it offers, smoothing has since seen numerous applications in quantum-enhanced parameter estimation tasks [26–32] and in estimating the outcomes of intermediate hidden measurements [33–35] and more recently has been framed in terms of generalized conditional estimators [36–38]. A form of quantum state smoothing similar to that in Ref. [1] was also studied by Budini [39,40]. Here we concentrate on the conceptual setup in Ref. [1].

Similarly to the classical state smoothing in Sec. III A, quantum state smoothing theory assumes a hidden Markov model with possible true (unknown) states, $\rho_T(t)$, consisting of only valid quantum states of the system. Importantly, these possible true states are not restricted to only orthogonal basis states as in the classical-like quantum smoothing. The goal is to obtain an estimated state $\check{\rho}(t)$ that is closest to possible true states. That is, the optimal estimate minimizes the expected cost function,

$$\mathcal{B}_{\mathbf{O}_C}[\check{\rho}] = \mathbb{E}_{\rho_T|\mathbf{O}_C}\{\mathcal{C}[\check{\rho}, \rho_T]\}, \tag{12}$$

where the average is taken over the set of possible true states $\mathbb{T}_t$. For the quantum case, we choose a trace-square deviation as the cost function as it is an analogue of the classical sum-square deviation in Eq. (2). The trace-square deviation is defined as

$$\mathcal{C}[\check{\rho}, \rho_T] = \mathrm{Tr}\left[(\check{\rho}(t) - \rho_T(t))^2\right]. \tag{13}$$

We can determine the estimator that minimizes this expected cost in a manner similar to that in the classical case. Setting to zero the derivative of Eq. (12) with respect to $\check{\rho}$ and solving for $\check{\rho}$, one obtains

$$\rho_C(t) = \mathbb{E}_{|\mathbf{O}_C}\{\rho_T(t)\}. \tag{14}$$

This yields the minimum value

$$\mathcal{B}^{\mathrm{TrSD}}_{\mathbf{O}_C}[\rho_C] = \mathbb{E}_{\rho_T|\mathbf{O}_C}\{P[\rho_T(t)]\} - P[\rho_C(t)], \tag{15}$$

where $P[\rho] = \mathrm{Tr}[\rho^2]$ is the purity of a state ρ. See Ref. [6] for an alternative derivation. If the conditioning "C" refers to the past observed record $\overleftarrow{\mathbf{O}}_t$, the optimal estimate is the filtered state $\rho_F(t) := \mathbb{E}_{|\overleftarrow{\mathbf{O}}_t}\{\rho_T(t)\}$. This is identical to the filtered state defined in standard quantum trajectory theory. When the conditioning is on both past and future records, $\overleftrightarrow{\mathbf{O}}$, the optimal estimate of the true state is given by

$$\rho_S(t) = \mathbb{E}_{|\overleftrightarrow{\mathbf{O}}}\{\rho_T(t)\}. \tag{16}$$

This is the definition of the smoothed quantum state, which, unlike the SWV state, is guaranteed to be a valid quantum state as it is a convex combination of valid quantum states.

It should be clear that, in general, it is the case that $\rho_S(t) \neq \rho_S^{\mathrm{cl}}$, due to the nonorthogonality of the set of true states $\mathbb{T}_t$. However, in the event that the possible true states are pure and mutually orthogonal, i.e., when $\mathbb{T}_t = \{|\psi_x\rangle\langle\psi_x| : \langle\psi_x|\psi_{x'}\rangle = \delta_{xx'}\}_{x=1}^{d}$, we have a "quantum-classical equivalence," $\rho_S(t) = \rho_S^{\mathrm{cl}}(t)$ [41]. Note that this quantum-classical equivalence is a sufficient condition only. However, at this point we have yet to specify how one can obtain the set of possible true states. Unlike in the classical state estimation, where possible true states can be directly associated with true configurations $\mathbf{x}_T(t)$ of the system, in the quantum state estimation, the definition of the set of possible true states $\mathbb{T}_t$ is subtler.

It is almost always the case that the observer, henceforth referred to as "Alice," does not have complete access to the environment into which the system is leaking information. (If she did, then the filtered state would, typically, be a pure state and no decrease in uncertainty from smoothing would be possible while a valid quantum state is maintained.) Thus, we consider a partition of the system's environment or baths into two parts. This applies even if, by conventional accounting, there is only one bath, if Alice's detection has some nonunit efficiency η. From this fraction of the bath, Alice's choice of measurement, $\mathcal{M}_A$, yields the measurement record $\mathbf{O}$, the "observed" record. For the remaining fraction, $1-\eta$ [42], this quantum information is *unobserved* by Alice. However, as it propagates away from the system, the information will encounter more complex environments that induce effectively irreversible decoherence. This defines a preferred basis [43,44] that can be regarded as a choice of measurement, $\mathcal{M}_B$ of the information, yielding a second measurement record $\mathbf{U}$ that is unobserved by Alice, called the "unobserved" record. We anthropomorphize this process by calling this "Bob's measurement and record."

With both these measurement records now defined, it is easy to see that the true state of the system is given by $\rho_T(t) = \rho_{\overleftarrow{\mathbf{O}}_t,\overleftarrow{\mathbf{U}}_t}$, as together the observed and unobserved measurement records contain the maximum amount of information about the system. This true state can be computed with standard quantum trajectory theory with measurements on multiple baths [14,15]. The set

of possible true states is then determined by the possible measurement records that could have occurred for Alice and Bob, given their respective measurement choice, i.e., $\mathbb{T}_t = \{\rho_{\overleftarrow{\mathbf{O}}_t \overleftarrow{\mathbf{U}}_t} | \mathcal{M}_A, \mathcal{M}_B\}_{\overleftarrow{\mathbf{O}}_t \overleftarrow{\mathbf{U}}_t}$. It is with this set that the smoothed quantum state was computed in previous studies [1,6,7,41].

One important thing to notice is that this definition for the set of true states explicitly depends on both Alice's and Bob's choice of measurement, as indicated by the notation $\mathbb{T}_t = \{\rho_{\overleftarrow{\mathbf{O}}_t \overleftarrow{\mathbf{U}}_t} | \mathcal{M}_A, \mathcal{M}_B\}_{\overleftarrow{\mathbf{O}}_t \overleftarrow{\mathbf{U}}_t}$. This dependence is expected, as we are dealing with quantum information, and it raises the question of how Bob's choice is determined. As stated above, we may consider Bob to be an anthropomorphic representation of the environment, rather than a real agent. In that case it is not possible to "ask" Bob what measurement he performed. Rather, one would have to infer the best model for how, ultimately, the quantum information from the system is turned into classical information by decoherence in the environment. However, for experimentally testing the theory, it would be necessary to have a "real" Bob—an agent who can potentially make different measurement choices $\mathcal{M}_B$, and reveal them to Alice (even while keeping the results from her). This is the situation we consider in the remainder of this paper. We stress again that while the choice of unraveling for Bob has no impact on the filtered quantum state, this choice can cause drastically different dynamics for the smoothed state [1,45,46].

IV. CLASSICAL-LIKE FILTERING AND RETROFILTERING DOES NOT GUARANTEE CLASSICAL-LIKE SMOOTHING

With the necessary background covered, we can move on to the main question this paper addresses. Say that for a given observed record $\overleftrightarrow{\mathbf{O}}$, Alice's filtered state and retrofiltered effect commute at all times, as in the experiments discussed above (see Sec. III D). Given only this, is it correct for Alice to use the classically smoothed estimate as her *optimal* smoothed estimate? If this proves true, it would open an entire regime where quantum state smoothing can be implemented without the need to know the measurement $\mathcal{M}_B$ that Bob performed. In particular, it might justify the approach already applied in the experiments detailed in Sec. III C. However, in the following sections we answer this question, and related questions, definitively in the negative. We address this in three stages, from which we obtain the following three results:

Result 1.—The commutativity of the filtered state and retrofiltered effect is not sufficient for the smoothed quantum state to reduce to its classical counterpart at time t. That is, $[\rho_F(t), \hat{E}_R(t)] = 0 \not\Rightarrow \rho_S(t) = \rho_S^{\mathrm{cl}}(t)$.

Result 2.—The commutativity of the filtered state and the retrofiltered effect is not sufficient for the smoothed state to mutually commute with both the filtered state and the retrofiltered effect.

Result 3.—The classical smoothed quantum state does not even always have the smallest expected cost function when compared with the smoothed state resulting from other unravelings for the environment.

We prove all these results using a single, very simple example open quantum system: a single two-level system (qubit) coupled to bosonic baths, the details of which are given in Sec. V. We then fix Alice's measurement choice (Sec. V A) so that the filtered state and the retrofiltered effect commute over a known time interval $[t_1, t_2)$. This is to ensure that we are always operating within the regime of interest for the question. For Bob's measurement, we investigate three potential choices for this. The first choice (Sec. V B) gives the classical regime, where his measurement is such that, over the interval (t_1, t_2), $\rho_T(t) \in \{|e\rangle\langle e|, |g\rangle\langle g|\}$, with $\langle e|g\rangle = 0$ causing $\rho_S(t)$ to equal $\rho_S^{\mathrm{cl}}(t)$. This case is considered first to provide a comparison for the following regimes. In the second (Sec. VI) and third (Sec. VII) cases, Bob's measurement is chosen so that $\rho_T(t)$ is not restricted to an orthogonal set over the interval (t_1, t_2). The second case considers a homodyne measurement of the output and enables us to prove Result 1. The third case considers an adaptive interferometric measurement strategy on the output bosonic field, and enables us to prove Result 2. For Result 3, in Sec. VIII, we investigate the expected cost functions of the smoothed quantum state in all three cases and show that for most of the time, the classical case yields a larger (and hence worse) estimate when compared with the other two cases.

V. MODEL: SINGLE QUBIT COUPLED TO EMISSION AND ABSORPTION CHANNELS

In this section we introduce the example system that is used throughout the remainder of this paper to prove our results. Also in this section we introduce the measurement that Alice makes on her portion of the environment, chosen so that the resulting filtered state and retrofiltered effect are mutually diagonal over the given time frame. This is to ensure that we are always operating within the regime where the filtered state and the retrofiltered effect are describable by a classical discrete hidden Markov model. Finally, in this section, we introduce the first choice for Bob's measurement, the one that explicitly realizes this hidden Markov model and so makes $\rho_S(t) = \rho_S^{\mathrm{cl}}(t)$. The two other, more complicated, measurement choices for Bob are explained in the subsequent sections.

The physical system we consider is a qubit that is coupled to three decoherence channels: two emission channels and one absorption channel. The dynamics of the quantum state, under no observation, is specified by a vector of

Lindblad operators,

$$\hat{\mathbf{c}} = (\sqrt{\delta}\hat{\sigma}_-, \sqrt{\gamma}\hat{\sigma}_-, \sqrt{\epsilon}\hat{\sigma}_+). \tag{17}$$

This defines the Lindblad master equation

$$\dot{\rho} = \mathcal{D}[\hat{\mathbf{c}}]\rho \equiv \sum_\ell \hat{c}_\ell \rho \hat{c}_\ell^\dagger - \{\hat{c}_\ell^\dagger \hat{c}_\ell, \rho\}/2, \tag{18}$$

as we are working in a frame where the system Hamiltonian disappears. In Eq. (17) we are using the Pauli ladder operators $\hat{\sigma}_\pm \equiv (\hat{\sigma}_x \pm i\hat{\sigma}_y)/2$, where $\hat{\sigma}_x$, $\hat{\sigma}_y$, and $\hat{\sigma}_z$ are the usual Pauli operators. We denote the eigenstates of $\hat{\sigma}_z$ by $\hat{\sigma}_z|e\rangle = |e\rangle$, $\hat{\sigma}_z|g\rangle = -|g\rangle$. The master equation (18) is extremely simple in this basis, looking like a classical bit stochastically transitioning between $|e\rangle$ and $|g\rangle$, which is described by the classical master equation for the ground state probability, $\wp(g;t) = \langle g|\rho(t)|g\rangle$,

$$\dot{\wp}(g;t) = (\delta + \gamma)\wp(e;t) - \epsilon\wp(g;t), \tag{19}$$

and the probability of being in the excited state being $\wp(e;t) = 1 - \wp(g;t)$.

A. Co-diagonal filtering and retrofiltering: Alice uses photon detection

Throughout, we consider the case where Alice perfectly monitors the first channel, corresponding to emission at rate δ. Since there is a second emission channel, with rate γ, we could imagine a single emission channel that Alice monitors with efficiency $\delta/(\delta+\gamma)$. To ensure Alice's filtered state and retrofiltered effect commute, over some time interval (t_1, t_2), it is sufficient to say that Alice uses photon detection to monitor her channel. Such a measurement, as shown shortly, causes both the filtered state and the retrofiltered effect to share the $\hat{\sigma}_z$ basis as their diagonal basis between any two detection events (jumps). The reader should see that the system and Alice's measurement we consider are isomorphic to the suggestive example in Fig. 1.

This measurement results in the following stochastic master equation for the filtered state [15]:

$$d\rho_F = \mathcal{G}[\hat{c}_o]\rho_F dN_o + \mathcal{D}[\hat{\mathbf{c}}_u]\rho_F dt - \frac{1}{2}\mathcal{H}[\hat{c}_o^\dagger \hat{c}_o]\rho_F dt, \tag{20}$$

with $\hat{c}_o = \sqrt{\delta}\hat{\sigma}_-$ and $\hat{\mathbf{c}}_u = (\sqrt{\gamma}\hat{\sigma}_-, \sqrt{\epsilon}\hat{\sigma}_+)$. The superoperators in Eq. (20) are $\mathcal{G}[\hat{a}]\rho = \hat{a}\rho\hat{a}^\dagger/\mathrm{Tr}[\hat{a}\rho\hat{a}^\dagger] - \rho$ and $\mathcal{H}[\hat{\mathbf{a}}]\rho = \sum_k \hat{a}_k\rho + \rho\hat{a}_k^\dagger - \mathrm{Tr}[\hat{a}_k\rho + \rho\hat{a}_k^\dagger]\rho$, and the stochastic increment characterizing the jump, dN_o, satisfies the following properties:

$$\mathbb{E}[dN_o] = \mathrm{Tr}[\hat{c}_o\rho\hat{c}_o^\dagger]dt, \qquad dN_o^2 = dN_o. \tag{21}$$

Here we have introduced the subscripts "o" and "u" to distinguish the channels observed and unobserved, respectively, by Alice.

To see that this measurement for Alice does result in a filtered state diagonal in the $\hat{\sigma}_z$ basis between any two consecutive jumps, we can compute Eq. (20) under a ground state initial condition given by the first jump at time t_1, i.e., $\rho_F(t_1^+) = |g\rangle\langle g|$ with $t_1^+ = t_1 + dt$, and a no-jump evolution $[dN_o(t) = 0]$. This results in $\rho_F(t) = \wp_F(e;t)|e\rangle\langle e| + \wp_F(g;t)|g\rangle\langle g|$, with $\wp_F(g;t)$ satisfying the differential equation

$$\dot{\wp}_F(g;t) = \gamma\wp_F(e;t) - \epsilon\wp_F(g;t) + \delta\wp_F(e;t)\wp_F(g;t), \tag{22}$$

and $\wp_F(e;t) = 1 - \wp_F(g;t)$

For the retrofiltered effect, the stochastic differential equation governing its evolution is [1,47]

$$-d\hat{E}_R = \tilde{\mathcal{G}}\left[\hat{c}_o^\dagger/\sqrt{\zeta}\right]\hat{E}_R dN_o + \mathcal{D}^\dagger[\hat{\mathbf{c}}_u]\hat{E}_R dt - \frac{1}{2}\tilde{\mathcal{H}}[\hat{c}_o^\dagger\hat{c}_o - \zeta]\hat{E}_R dt, \tag{23}$$

which is evolved backwards in time from the final condition $\hat{E}_R(t_f) \propto \hat{1}$, representing a final uninformative state. In Eq. (23), $\tilde{\mathcal{G}}[\hat{a}]\rho = \hat{a}\rho\hat{a}^\dagger - \rho$ and $\tilde{\mathcal{H}}[\hat{\mathbf{a}}]\rho = \sum_k \hat{a}_k\rho + \rho\hat{a}_k^\dagger$ are the linear versions of the nonlinear superoperators introduced above, while ζ is an arbitrary positive constant that affects only the norm of $\hat{E}_R$. It is related to a so-called ostensible probability distribution for jumps; see Ref. [47]. Thus, strictly, $\hat{E}_R$ is only proportional to the effect, but all the expressions for the smoothed state are normalized so that the norm of $\hat{E}_R$ for a fixed $\overrightarrow{\mathbf{O}}_t$ does not matter.

Now we show that the retrofiltered effect is also diagonal in the $\hat{\sigma}_z$ basis between any two consecutive observed jumps. We have the final condition at the time just before the second jump t_2 that $\hat{E}_R(t_2^-) \propto |e\rangle\langle e|$, where $t_2^- = t_2 - dt$. To see this, one can use the quantum map form for the evolution of the retrofiltered effect (see Appendix A for an explanation),

$$\hat{E}_R(t_2^-) = \hat{M}_o^\dagger(\mathbf{y}_o;t_2)\sum_{\mathbf{y}_u}\hat{M}_u^\dagger(\mathbf{y}_u;t_2)\hat{E}_R(t_2) \times \hat{M}_o(\mathbf{y}_u;t_2)\hat{M}_o(\mathbf{y}_o;t_2). \tag{24}$$

Since at t_2 a photon is detected in the δ channel, the map corresponding to the observed measurement takes the form $\hat{M}_o(\mathbf{y}_o;t_2) \propto \hat{c}_o \propto |g\rangle\langle e|$. Computation of Eq. (24) with this map yields the final condition for the effect. Computing the evolution of the retrofiltered effect given this final condition at t_2^- and under a no-jump evolution $(dN_o = 0)$, we obtain the solution $\hat{E}_R(t) = E_R(e;t)|e\rangle\langle e| +$

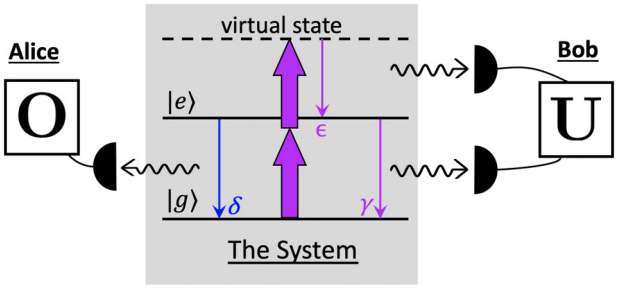

FIG. 2. A qubit undergoing three separate dynamical processes. The first two processes are photon emission processes, one with rate δ that is monitored by Alice (blue arrow) using photon detection and one with rate γ monitored by Bob, again using photon detection. The final process is an absorption process with rate ϵ, modeled by continuous two-photon driving (large purple arrows) to a virtual state that immediately decays to the excited state via photon emission, that is observed by Bob via photon detection.

$E_R(g;t)|g\rangle\langle g|$, where the coefficients satisfy

$$\dot{E}_R(g;t) = \epsilon\big(E_R(g;t) - E_R(e;t)\big) + \zeta E_R(g;t),$$
$$\dot{E}_R(e;t) = \gamma\big(E_R(e;t) - E_R(g;t)\big) + (\delta+\zeta)E_R(e;t). \tag{25}$$

Thus, by Alice choosing photon detection, from her perspective, the quantum system can be completely described by a classical hidden Markov model between any two detection events. This means that the entire evolution has this nature apart from potentially the evolution before the first jump if the initial state is not diagonal in the $\hat{\sigma}_z$ basis.

As Bob monitors all the channels that Alice's measurement missed, this leaves him to perfectly monitor the γ and ϵ channels. One might be wondering how it is possible for Bob to measure an absorption channel. Up until now we have not provided details about how the absorption channel could have arisen physically. We consider that the qubit is under continuous two-photon driving of a Raman transition [48–51] to a virtual state that immediately decays to the excited state by emitting a (detectable) photon; see Fig. 2. Such a scheme can be made equivalent to an absorption channel with rate ϵ while emitting a photon of a frequency different from those in the emission channels so that it can be monitored, similarly to the emission channel, by detecting this photon. With this technical point taken care of, we next turn to Bob's first choice of measurement.

B. Classical smoothed state: Bob uses photon detection

In this section we want Bob's measurement to be such that $\mathbb{T}_t = \{|g\rangle\langle g|, |e\rangle\langle e|\}$ for all $t \in (t_1, t_2)$, with $\rho_T(t_1^+) = |g\rangle\langle g|$. Just as for Alice, above, this is easy to achieve by having Bob monitor the remaining two channels perfectly using photon detection. For this measurement scheme, the stochastic master equation for the true state is [15]

$$d\rho_T = \mathcal{G}[\hat{c}_o]\rho_T dN_o - \frac{1}{2}\mathcal{H}[\hat{c}_o^\dagger\hat{c}_o]\rho_T dt + \mathcal{G}[\hat{c}_{u,\gamma}]\rho_T dN_{u,\gamma} - \frac{1}{2}\mathcal{H}[\hat{c}_{u,\gamma}^\dagger\hat{c}_{u,\gamma}]\rho_T dt + \mathcal{G}[\hat{c}_{u,\epsilon}]\rho_T dN_{u,\epsilon} - \frac{1}{2}\mathcal{H}[\hat{c}_{u,\epsilon}^\dagger\hat{c}_{u,\epsilon}]\rho_T dt, \tag{26}$$

where $dN_{u,k}$ are the stochastic increments describing the detection of a photon in the corresponding channel.

To see that this measurement choice of Bob does indeed result in the true state being in either the ground state or the excited state between any two consecutive observed jumps, we can look at each term in Eq. (26) individually. Firstly, as we are considering the evolution between two consecutive observed jumps, we know that initially the true state will be in the ground state and that $dN_o(t) = 0$ until the following jump, removing the first term in Eq. (26). Leaving the terms of order dt for last, we find the remaining unobserved jump terms project the true state into either the ground state or the excited state if a photon is detected in either the γ channel or the ϵ channel, respectively. Finally, looking at the terms of order dt, when computing these with the system in the ground state, we find they are equal to zero. This means that the true state will remain in the ground state until a photon is detected in the ϵ channel and projects it into the excited state. Computation of the dt terms also gives zero when the true state is in the excited state and it remains unchanged until it is projected into the ground state via an emission of a photon in the γ channel. Thus, under this monitoring by Bob, the true state between any two observed jumps will be in either only the ground state $|g\rangle\langle g|$ or only the excited state $|e\rangle\langle e|$, as claimed.

With $\mathbb{T}_t$ obtained, all that remains is to compute the smoothed quantum state. For this case it is a fairly simple task. Beginning with Eq. (16), we have

$$\begin{aligned}\rho_S(t) &= \sum_{m\in\{g,e\}} \wp(m;t|\overleftrightarrow{\mathbf{O}})|m\rangle\langle m| \\ &\propto \sum_{m\in\{g,e\}} \wp(\overrightarrow{\mathbf{O}}_t|m,t)\wp(m;t|\overleftarrow{\mathbf{O}}_t)|m\rangle\langle m| \\ &= \sum_{m\in\{g,e\}} \mathrm{Tr}\Big[\hat{E}_R(t)|m\rangle\langle m|\Big]\wp(m;t|\overleftarrow{\mathbf{O}}_t)|m\rangle\langle m| \\ &= E_R(g;t)\wp_F(g;t)|g\rangle\langle g| + E_R(g;t)\wp_F(g;t)|e\rangle\langle e|,\end{aligned} \tag{27}$$

where we have used Bayes' theorem in the second line and in the final line we have recognized that $\wp(m;t|\overleftarrow{\mathbf{O}}_t)$ is exactly the coefficient for the filtered state in Eq. (22). After normalization this gives $\rho_S(t) = \wp_S(e;t)|e\rangle\langle e| + \wp_S(g;t)|g\rangle\langle g| = \rho_S^{\mathrm{cl}}(t)$, as expected.

For a simpler analysis, we henceforth consider the case where $\delta \to 0^+$. In this limit, Alice very rarely observes a jump causing (t_1, t_2) to, typically, be large enough for both the filtered state and the retrofiltered effect to reach their respective stationary solutions between any two consecutive jumps. As a result, the filtered state and the smoothed quantum state differ only for a time on the timescale that the system equilibrates, in this case $1/(\gamma + \epsilon)$, before the final jump. To see why this is the case, we need to look at the retrofiltered effect. From Eq. (25), the steady-state solution is $E_R^{\mathrm{SS}}(e) = E_R^{\mathrm{SS}}(g) = \lambda(t)$, where $\lambda(t)$ is half the norm of $\hat{E}_R$. (Recall that the norm does not affect any calculated quantities, and so it can be time dependent even in the steady state.) This means that whenever the retrofiltered effect is in the steady state, the smoothed quantum state in Eq. (27), when normalized at time t, will be equal to the filtered state. Thus, in the limit $\delta \to 0^+$, the retrofiltered effect will be in the steady state over the entire evolution until a time of order $1/(\gamma + \epsilon)$. Thus, we need to consider only the evolution of the state on this timescale before an observed jump.

To gain some physical understanding of $\rho_S^{\mathrm{cl}}(t)$ in this system, let us compare it with the filtered state. We can see in Fig. 3(a) that, unsurprisingly, before the jump occurring at $t = 0$, the filtered state (solid blue line) remains in its steady state $\wp_F^{\mathrm{SS}}(e) = \epsilon/(\gamma + \epsilon)$ until the jump, whereupon it is projected into the ground state. The smoothed quantum state (dashed green line), on the other hand, begins to diverge from the filtered state as the jump approaches and just before the jump reaches the excited state before it is projected to the ground state. This divergence is expected as the smoothed state "knows" that a jump is about to occur, as it is conditioned on the future measurement record. Furthermore, since the true state can be in either the ground state or the excited state, this means that for a jump to occur, the system must have been in the excited state.

If we look at the purity of the filtered state and the smoothed quantum state in Fig. 3(b), we see that as the smoothed quantum state begins to deviate from the filtered state, the purity begins to drop rapidly. Such a drop is not surprising as for the smoothed state to reach the excited state it must pass through the maximally mixed state, resulting in the smoothed quantum state having minimal purity before the jump. However, this brings up an interesting point. From Eq. (15), we know that the expected cost function for the optimal state is equal to the average difference between the purity of the true state and purity of the conditioned state. However, for this system, the true state is pure irrespective of the unobserved measurement record, and Eq. (15) reduces to the impurity of the conditioned state. This means that since the purity of the smoothed state decreases below that of the filtered state just before the jump, the filtered state seemingly gives a lower expected cost function and would be the optimal estimator of the true state, not the smoothed quantum state. However, this is not true, as stated earlier and proved in Ref. [6].

The issue lies in how the expected cost function is calculated for the filtered state. Use of Eq. (15) for the filtered state assumes that one has access only to Alice's past measurement record, whereas the smoothed quantum state assumes that the past-future record is available. Thus, to compare the expected cost function of the filtered state with that of the smoothed state, one must take the future measurement record into account and compute

$$\mathcal{B}_{\mathbf{O}_S}^{\mathrm{TrSD}}[\rho_F] = 1 - 2\mathrm{Tr}[\rho_F \rho_S] + P(\rho_F). \tag{28}$$

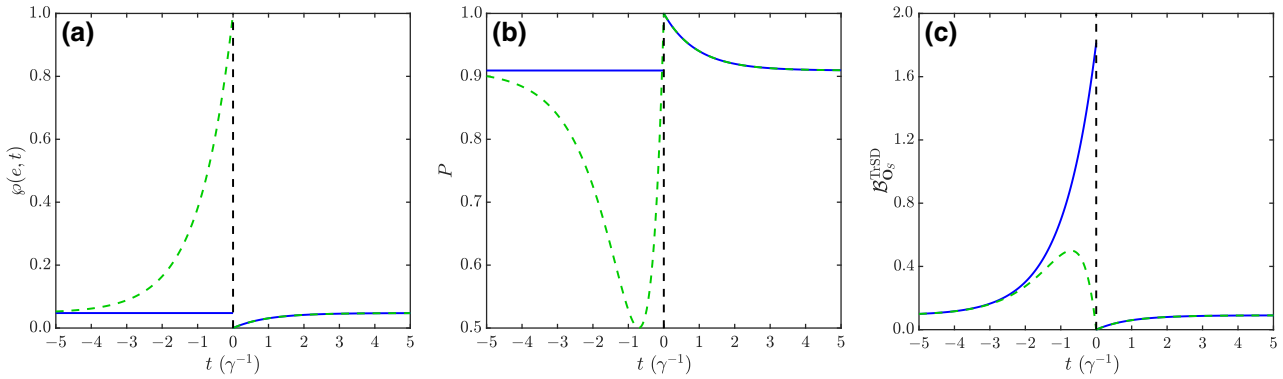

FIG. 3. (a) Filtered probability (blue line) and smoothed the probability (dashed green line) of the system being in the excited state. Before the jump (at time $t = 0$), the smoothed state begins to increase until it reaches unity immediately before the jump. (b) Purity of the filtered and smoothed states. The purity of the smoothed state begins to decrease before the jump due to the state having access to the future measurement record. (c) Past-future expected cost function for the filtered state, obtained with Eq. (28), and the smoothed state, obtained with Eq. (15). The expected cost for the smoothed estimate of the state is seen to be a better estimator than the filtered estimate due to its smaller expected cost before the jump. In all cases, we have taken $\epsilon = 0.05\gamma$ and the limit $\delta \to 0^+$. Time t has units of γ^{-1}.

Note that this argument also holds for classical systems, with the appropriate analogues of the states and cost function. When computing the expected cost function of the filtered state in this way, we see, in Fig. 3(c), that the smoothed quantum state has the lower expected cost function.

VI. PROOF OF RESULT 1: BOB USES X HOMODYNE MEASUREMENTS

In this section we prove, by considering a different measurement choice for Bob, that the smoothed quantum state need not equal the classically smoothed quantum state. Here, instead of photon detection, Bob (perfectly) monitors the unobserved channels each with homodyne measurements. That is, the output light of the system is combined with a local oscillator with phase φ on a 50:50 beam splitter, at which point both outputs of the beam splitter are measured with photon detectors. The single two signals are then subtracted, yielding quadrature information about the system. See Fig. 4. Specifically, the measurement current obtained is given by [15,47]

$$J_k dt = \langle \hat{c}_{u,k} e^{i\varphi_k} - \hat{c}^\dagger_{u,k} e^{-i\varphi_k} \rangle dt + dW_k, \tag{29}$$

where $k = \gamma, \epsilon$, φ_k is the local oscillator phase for the k channel, and dW_k is the innovation, an infinitesimal Wiener increment satisfying

$$\mathbb{E}\{dW_k\} = 0, \quad dW_k dW'_k = \delta_{kk'} dt. \tag{30}$$

Such monitoring causes the true state to evolve according to the stochastic master equation [15]

$$d\rho_T = \mathcal{G}[\hat{c}_o]\rho_T dN_o - \frac{1}{2}\mathcal{H}[\hat{c}^\dagger_o \hat{c}_o]\rho_T dt + \mathcal{D}[\hat{\mathbf{c}}_u]\rho_T dt + \mathcal{H}[\hat{\mathbf{c}}_\phi d\mathbf{W}]\rho_T, \tag{31}$$

where $\hat{\mathbf{c}}_\varphi = [\hat{c}_{u,\gamma} e^{i\varphi_\gamma}, \hat{c}_{u,\epsilon} e^{i\varphi_\epsilon}]$ and $d\mathbf{W} = [dW_\gamma, dW_\epsilon]^\top$. From this point forward, we consider the case where $\varphi_\gamma = \varphi_\epsilon = 0$, i.e., X homodyne measurements on both channels. Note that this is called an "X homodyne measurement" since the measurement current contains information only about the x component of the Bloch vector $\mathbf{r} = (x, y, z)^\top$ that characterizes the state of the qubit, where $\rho = \frac{1}{2}(\hat{1} + \mathbf{r} \cdot \hat{\boldsymbol{\sigma}})$ and $\hat{\boldsymbol{\sigma}} = (\hat{\sigma}_x, \hat{\sigma}_y, \hat{\sigma}_z)^\top$. The analysis that follows would also hold in this system for any choice of homodyne phase $\varphi_\gamma = \varphi_\epsilon = \varphi$.

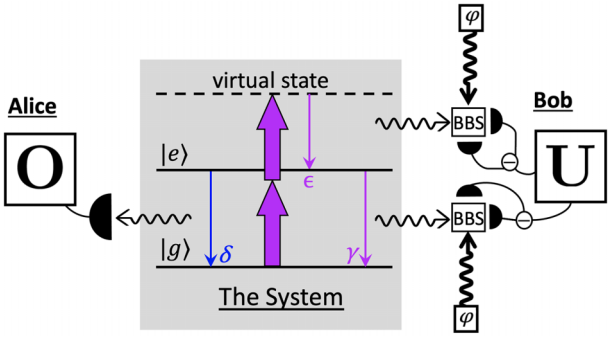

FIG. 4. Same physical system as in Fig. 2 with Bob now measuring his γ and ϵ channels both (independently) using X homodyne measurements (with local oscillator phase $\varphi = 0$). BBS, balanced beam splitter.

The important point about this measurement scheme for Bob is that between two observed jumps, ρ_T is not restricted to the set $\{|g\rangle\langle g|, |e\rangle\langle e|\}$, but instead can be in any pure state on the x-z great circle of the Bloch sphere. The true state is pure between jumps because it starts in the (pure) ground state and remains pure since the system is perfectly monitored by both Alice and Bob. The pure state can be confined to the x-z great circle of the Bloch sphere because without Bob's measurement, the quantum state is confined to the z axis of the Bloch sphere and conditioning on an X homodyne measurement will give information only about the x component of the Bloch vector. Hence, the true state will, typically, have a nonzero x component, while the y component will remain zero.

To prove this more rigorously, one can obtain the stochastic differential equations for the Bloch vector of the true state from Eq. (31) subject to the initial condition $\rho_T(t_1^+) = |g\rangle\langle g|$ and a no-jump record $dN_o(t) = 0$. We again take the limit $\delta \to 0^+$ to simplify the computation. For this measurement scenario we have

$$dz = [-\gamma(1+z) + \epsilon(1-z)]\,dt - \sqrt{\gamma}x(1+z)dW_\gamma + \sqrt{\epsilon}x(1-z)dW_\epsilon, \tag{32}$$

$$dy = y\left[-\frac{1}{2}(\gamma+\epsilon)dt - \sqrt{\gamma}x dW_\gamma - \sqrt{\epsilon}x dW_\epsilon\right], \tag{33}$$

$$dx = -\frac{1}{2}(\gamma+\epsilon)x dt + \sqrt{\gamma}(1+z-x^2)dW_\gamma + \sqrt{\epsilon}(1-z-x^2)dW_\epsilon, \tag{34}$$

with $z(t_1^+) = -1$ and $y(t_1^+) = x(t_1^+) = 0$. With these equations we see that, due to the initial condition, the y component will remain zero until the next observed jump.

Since the true state is restricted to the x-z great circle, we can reparametrize the true state by the angle θ of y rotation from the positive z axis instead of the Bloch vector. That is, defining

$$\rho_T(\theta; t) = \frac{1}{2}(\hat{1} + \sin\theta(t)\hat{\sigma}_x + \cos\theta(t)\hat{\sigma}_z), \tag{35}$$

we have $\mathbb{T}_t = \{\rho_T(\theta; t) : \theta \in [0, 2\pi)\}$ for all $t \in (t_1, t_2)$. With this θ parametrization, we can reduce the evolution of the true state between two observed jumps to a single stochastic differential equation for θ. Using the Itô formula

[15,52] to move from a differential equation in $\cos\theta$ (or $\sin\theta$) to one in θ, we obtain

$$d\theta = A(\theta)dt + B_\gamma(\theta)dW_\gamma + B_\epsilon(\theta)dW_\epsilon, \tag{36}$$

where $A(\theta) = \sin\theta[\frac{1}{2}(\gamma+\epsilon)\cos\theta + (\gamma-\epsilon)]$, $B_\gamma(\theta) = \sqrt{\gamma}(1+\cos\theta)$, and $B_\epsilon(\theta) = -\sqrt{\epsilon}(1-\cos\theta)$.

We can now begin to compute the smoothed quantum state for this case. From Eq. (16), we have

$$\begin{aligned}\rho_S(t) &= \int_0^{2\pi} \wp(\theta;t|\overleftrightarrow{\mathbf{O}})\rho_T(\theta)d\theta \\ &\propto \int_0^{2\pi} \mathrm{Tr}[\hat{E}_R(t)\rho_T(\theta)]\wp(\theta;t|\overleftarrow{\mathbf{O}}_t)\rho_T(\theta)d\theta. \end{aligned}\tag{37}$$

As we are considering only the evolution between two observed jumps, we only need to find $\wp(\theta;t|\overleftarrow{\mathbf{O}}_t) = \wp(\theta;t|\overleftarrow{\mathbf{O}}_{\mathrm{NJ}})$, as the retrofiltered effect can be computed via Eq. (23). Here the conditioning $\overleftarrow{\mathbf{O}}_{\mathrm{NJ}}$ stands for a no-jump record. Since Eq. (36) is in the form of a Langevin equation, it can be mapped to a Fokker-Planck equation [7,15,52,53] describing the evolution of the probability density of θ for unknown Wiener processes. However, since Eq. (36) assumes a no-jump observed record, the probability density the Fokker-Planck equation describes is $\wp(\theta;t|\overleftarrow{\mathbf{O}}_{\mathrm{NJ}})$. For this Langevin equation, the corresponding Fokker-Planck equation is

$$\begin{aligned}\partial_t\wp(\theta;t|\overleftarrow{\mathbf{O}}_{\mathrm{NJ}}) &= -\partial_\theta A(\theta)\wp(\theta;t|\overleftarrow{\mathbf{O}}_{\mathrm{NJ}}) \\ &\quad + \frac{1}{2}\sum_{k\in\{\gamma,\epsilon\}}\partial_\theta^2 B_k(\theta)^2\wp(\theta;t|\overleftarrow{\mathbf{O}}_{\mathrm{NJ}}), \end{aligned}\tag{38}$$

where $\partial_x = \partial/\partial x$, with the initial condition $\wp(\theta;t_1^+|\overleftarrow{\mathbf{O}}_{\mathrm{NJ}}) = \delta(\theta-\pi)$ corresponding to the ground state and the boundary condition $\wp(0;t|\overleftarrow{\mathbf{O}}_{\mathrm{NJ}}) = \wp(2\pi;t|\overleftarrow{\mathbf{O}}_{\mathrm{NJ}})$. We solve this Fokker-Planck equation numerically using MATHEMATICA's NDSolve function with a Gaussian initial condition $g(\theta;\mu=\pi,V=0.01\gamma)\approx\delta(\theta-\pi)$, where the mean of the Gaussian is μ and the variance is V. With the probability density found, we can now compute the smoothed quantum state in the X homodyne case for comparison with the photon detection case.

As an aside, in general, calculation of the smoothed quantum state requires use of an ensemble of unnormalized true states generated according to an ostensible probability distribution; see, for example, Refs. [7,47]. That is, one must calculate an extra stochastic variable, the norm of each possible true state. This applies, in general, even in the current simple system, where we can generate the ensemble of true states by solving a Fokker-Planck equation. Specifically, the Fokker-Planck equation must be modified to describe the joint probability of θ and the normalization [7,53]. In the present case, however, since we are considering the limit $\delta\to 0^+$, the amount of information Alice gains from a no-detection event is negligible, as this is almost always the result, causing the equation of the true state to reduce to just the unobserved evolution. Since the actual probabilities, for this case, can be computed easily from the distributions for dW_γ and dW_ϵ, the normalized equation for the true state can be used.

We can now begin to compute the smoothed quantum state. We can see that in this homodyne case, the smoothed quantum state will be diagonal in the $\hat{\sigma}_z$ basis because of a symmetry in the dynamics. Specifically, since there are no unitary dynamics driving the system in a particular way, for any unobserved measurement record that causes the true state to rotate clockwise on the x-z great circle, there is an equally likely record of the opposite sign that causes the state to evolve in exactly the same way in the counterclockwise direction. Importantly, it is equally likely even given the future record (the jump) that Alice observes because the excited state probability is the same for both directions of rotation. Thus, when Alice averages over the possible unobserved records, each true state can be paired with its mirror image about the z axis, canceling the x component of the Bloch vector.

We can thus easily compare the X homodyne smoothed quantum state with the classically smoothed quantum state by looking only at their z components. As Fig. 5 shows,

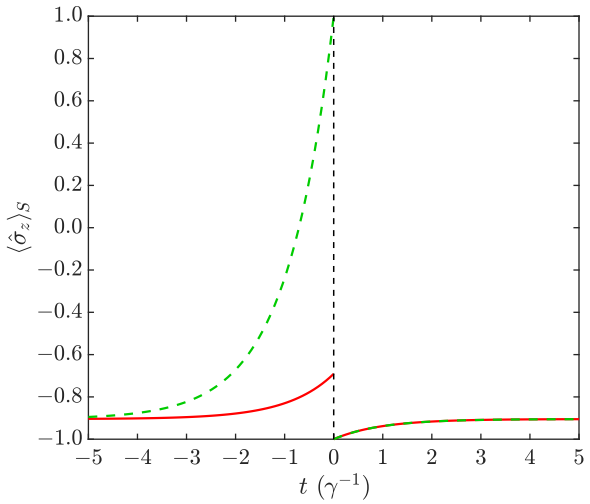

FIG. 5. Comparison of the conditional average of the z component of the Bloch vector when Alice's measurement record is obtained by photon detection and Bob's measurement record is obtained by either photon detection (dashed green line) or an X homodyne measurement (red line). Here we have taken $\delta\to 0^+$ and $\epsilon = 0.05\gamma$ and an observed detection (jump) occurs at time $t=0$. The z component for the smoothed state with an X homodyne measurement for Bob differs from the classically smoothed state despite the filtered state being diagonal in the $\hat{\sigma}_z$ basis, proving Result 1. Time t has units of γ^{-1}.

there is a clear difference between them. [As explained in Sec. V B, in the limit $\delta \to 0^+$ we need be concerned only with the smoothed quantum state in a time of order $1/(\gamma + \epsilon)$ before the final jump.] Thus, by this example, we have proven Result 1: the commuting of the filtered state and the retrofiltered effect is *not* sufficient for $\rho_S(t)$ to equal $\rho_S^{\mathrm{cl}}(t)$.

In this example, the obvious difference between the smoothed state obtained classically (when Alice assumes an orthogonal basis for the true state) and that obtained when Bob performs a homodyne measurement (when Alice takes this into account) is the value of z for the smoothed state immediately before the jump. We can intuitively understand this as follows. Since the true state in the latter case can be in a superposition of both the ground state and the excited state, as opposed to being in only one of these states, a jump can occur even when the system is not in the excited state. Thus, when Alice is estimating the true state using smoothing, she cannot be certain that the true state was in the excited state just before the transition, unlike in the classical (photon detection) case, where she is certain. Therefore, her smoothed estimate in the homodyne case moves somewhat closer to the excited state only as the jump approaches.

VII. PROOF OF RESULT 2: BOB USES AN ADAPTIVE MEASUREMENT

In the preceding section, the nonclassical smoothed state was still diagonal in the same basis as the classical smoothed state, and therefore diagonal in the same basis as the filtered state and the retrofiltered effect (whose co-diagonality defines the scenario we are investigating). In this section we show the stronger result that the smoothed quantum state is not necessarily even co-diagonal with ρ_F and $\hat{E}_R$. As we saw in the X homodyne example, the smoothed quantum state was diagonal in the $\hat{\sigma}_z$ basis because Bob's measurement gave the set of possible true states a symmetry about the z axis of the Bloch sphere. To avoid reasoning of this sort for this final case, Bob's measurement is chosen to break this symmetry in the set of possible true states.

To achieve an asymmetric distribution of true states, we allow Bob to use an adaptive measurement involving finite-strength local oscillators on the unobserved channels; see Fig. 6. Here, "finite strength" means that the local oscillator intensity is comparable to the intensity of light emitted by the system, so the detection still resolves individual photons (unlike the strong local oscillator case of a homodyne measurement). The measurement is "adaptive" in the sense that after every detection event, the amplitude (strength and phase) of the local oscillators can be changed, depending on the current settings of these amplitudes and the type of photon detection that occurs (if more than one detector is used, which is the case for our system here, with two unobserved channels). Measurements of

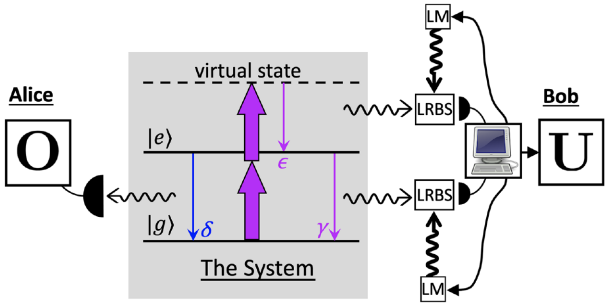

FIG. 6. Same physical system as in Fig. 2 with Bob using the adaptive measurement scheme in Appendix B. LM, light modulator; LRBS, low-reflectivity beam splitter.

this kind have been studied theoretically for many decades [54–58].

A nontrivial property of adaptive measurements of the sort described is that they can constrain the stochastic evolution of the true state of the system to a finite and time-independent set $\mathbb{T}$. Note the lack of a subscript t. Together with the corresponding stationary probabilities of each state in $\mathbb{T}$, this comprises a so-called *physically realizable ensemble* (PRE) [59]. The significance of "physically realizable" here is as follows. Consider a Markovian (in the strongest sense [60]) open quantum system whose unconditional evolution is described by a Lindblad master equation, where in the long-time limit, $t \geq t^{\mathrm{SS}}$, the system reaches a unique stationary solution that is mixed. Because a mixed quantum state can be decomposed into a weighted ensemble of pure states in infinitely many ways, there are different interpretations of how the underlying pure state dynamics of the system unfold. However, only some of these pure state ensembles are physically realizable, meaning that there exists a way to continuously monitor the environment (without affecting the unconditional evolution) such that the conditioned state at times after t^{SS} is confined to $\mathbb{T}$, with the corresponding probabilities being realized in the ergodic sense.

The classical ensemble in Sec. V B, with $\mathbb{T} = \{|g\rangle\langle g|, |e\rangle\langle e|\}$, is an example of such a PRE, but in general the states in $\mathbb{T}$ need not be orthogonal [56–58]. This is essential for finding an asymmetric (under application of $\hat{\sigma}_z$) steady-state ensemble. [In our case, this steady state means a long time, compared with $1/(\gamma + \epsilon)$, after Alice's last jump, which is always the limit we can consider when Alice's jump rate $\delta \to 0^+$; see more below.] For our system, the particular adaptive measurement scheme is chosen so that $\mathbb{T}$ comprises three states, with no symmetry under application of $\hat{\sigma}_z$. The conditioned dynamics causes the true state to cyclically transition between these states. This is possible only in certain parameter regimes, which is why we chose $\epsilon = 0.05\gamma$.

A detailed discussion of PREs in the context of the photon emission and absorption master equation is given in

Ref. [57, Sec. 4.4.2] In our case, the scenario is modified slightly as it is Bob's measurement record that causes Alice's filtered state (as opposed to the unconditioned state) to become pure upon conditioning. That is, we make the substitution $\rho \to \rho_F$ and it is Bob's measurement that causes the true state to become pure when we are deriving the PRE for the system. Note that there is a subtlety in regard to the filtered state that one should be aware of when making this substitution. In the standard PRE scenario, it is necessary for the unconditioned state to have reached a unique stationary solution. However, the filtered state is a stochastic quantity and, in general, will not reach a unique stationary solution in the long-time limit. Therefore, there are only select cases, i.e., when the filtered state (or some deterministic property of the state [41]) reaches a unique steady state, where we can apply the PRE theory in this manner.

In the example that we consider, such a steady state will usually exist for the filtered state, provided the time between consecutive jumps, τ, is typically much longer than the time in which the system equilibrates; more formally, when $\tau = (\delta\langle e|\rho|e\rangle)^{-1} \gg (\gamma + \epsilon + \delta)^{-1}$. Since after the first jump, $\rho(t_1) = |g\rangle\langle g|$, it will always be the case that $\langle e|\rho|e\rangle \leq \langle e|\rho^{\mathrm{SS}}|e\rangle = \epsilon(\gamma + \epsilon + \delta)^{-1}$. Thus, the filtered state is likely to reach the steady state between consecutive jumps if we operate in the parameter regime

$$\delta\epsilon \ll (\gamma + \epsilon + \delta)^2 \approx (\gamma + \epsilon)^2, \tag{39}$$

where, for the final approximation, we have assumed $\delta \ll \gamma + \epsilon$. Note that for the parameter regime we have been considering thus far ($\epsilon = 0.05\gamma$), we require that $\delta \ll 22\gamma$. As has been the case for the other measurement scenarios, we, for simplicity, take the limit $\delta \to 0^+$. For the stationary solution of the filtered state in this example,

$$\rho_F^{\mathrm{SS}} = \frac{\epsilon}{\gamma + \epsilon}|e\rangle\langle e| + \frac{\gamma}{\gamma + \epsilon}|g\rangle\langle g|, \tag{40}$$

the cyclic physically realizable ensemble $\{\rho(\theta), \wp_\theta\}_{\theta\in\{\alpha,\beta,\phi\}}$ chosen, from the possible valid ensembles, is displayed in Fig. 7 with the angles and corresponding probability weights. It should be emphasized that the implemented measurement strategy [57] causes only the true state to undergo the cyclical dynamics depicted in Fig. 7 when the filtered state is in steady state. Outside this regime, the dynamics of the true state may be more complicated but when averaged still result in the transient dynamics of the filtered state. The reader is referred to Appendix B for the local oscillator settings that achieve the PRE shown in Fig. 7.

With the measurement scheme and dynamics of the true quantum state covered, we can now begin to compute the

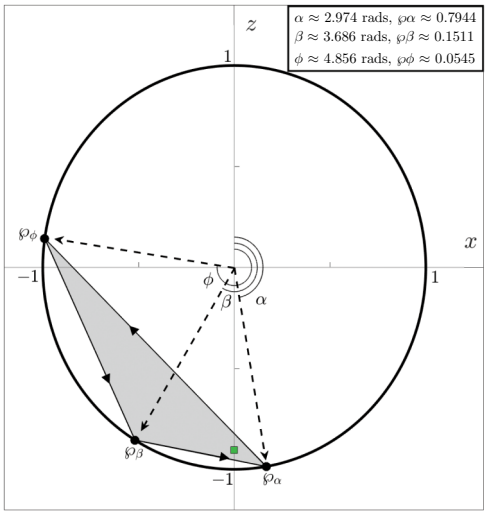

FIG. 7. x-z great circle of the qubit's Bloch sphere showing the cyclic physically realizable ensemble chosen for the example qubit system subjected to the measurement scheme in Fig. 6 plotted on the x-z great circle. The three black points on the circle are the three pure states in the ensemble, with there corresponding angles and occupation probabilities given in the top-right corner (see Ref. [57] for how these are calculated) and the arrows connecting them showing the cyclic dynamics that results from the adaptive measurement strategy. The shaded region is where both the filtered state and the smoothed quantum state must reside at times after t^{SS}. The green square indicates ρ_F^{SS}. See Fig. 5 for the parameter details.

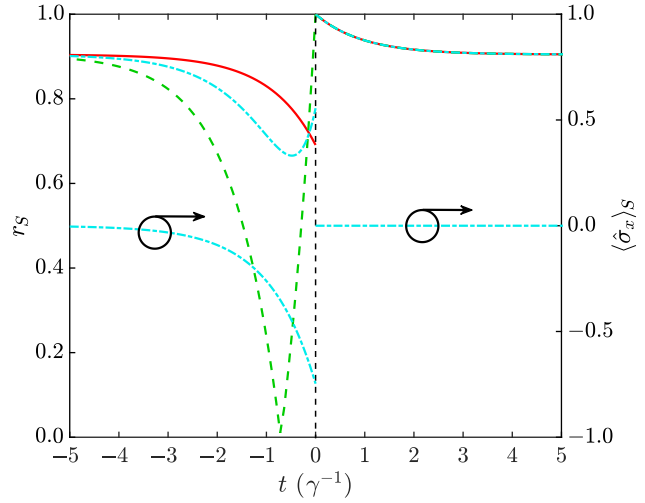

FIG. 8. Length (left-hand-side axis) and x component (right-hand-side axis) of the Bloch vector for the smoothed quantum state when Alice's measurement record is obtained by photon detection and Bob's measurement record is obtained by photon detection (dashed green line), an X homodyne measurement (solid red line), or an adaptive weak local oscillator strategy (dot-dashed cyan line). The x components of the smoothed state when Bob implements photon detection or an X homodyne measurement are not shown as they are zero at all times. The looped arrows indicate that the line within the loop belongs to the right axis. Time t has units of γ^{-1}.

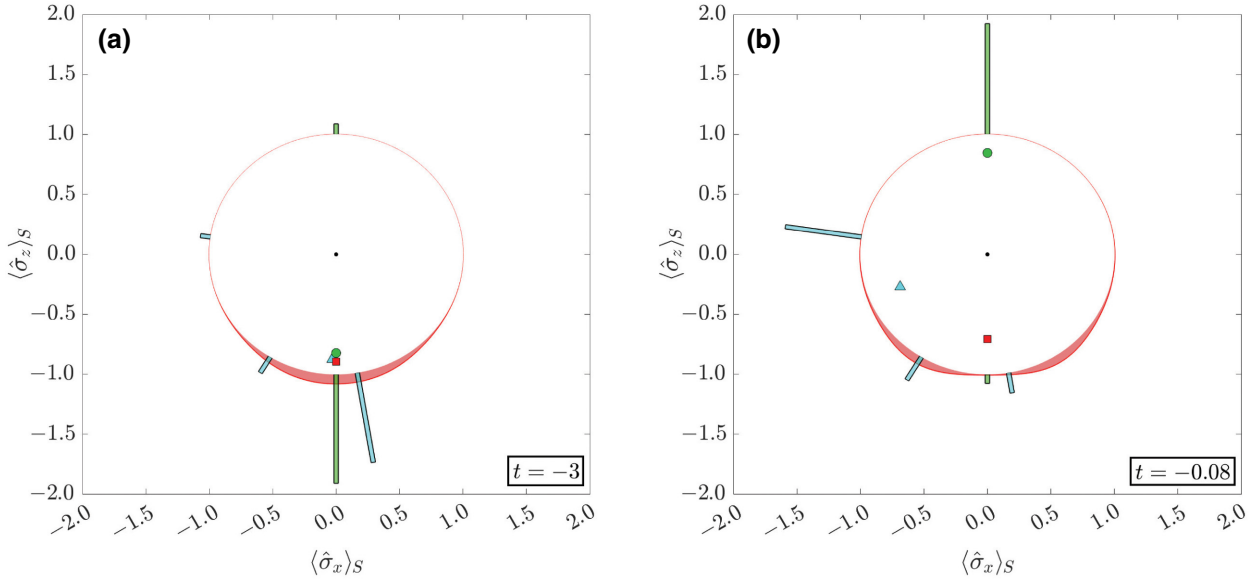

FIG. 9. x-z great circles of the Bloch sphere plotted at two different times before the observed jump. On the surface of the circle, the probability distributions are plotted for the case where Bob measures the environment using photon detection (green), an X homodyne measurement (red), and an adaptive scheme (cyan) (all of which have a zero y component). The relative area of the bars indicates the occupation probability for that state. Note that the total areas of the green and cyan bars are equal but the area under the red curve has been scaled by a factor of 3 for clarity. The markers (circle, square and triangle) in the interior correspond to the smoothed mean of the Bloch vector using the correspondingly colored distribution. See Fig. 5 for the parameter details.

smoothed quantum state for this case. As in the previous two cases, the smoothed quantum state differs from the filtered state only for a time of order $1/(\gamma+\epsilon)$ before the second observed jump. Therefore, we need to compute the smoothed quantum state only when the retrofiltered effect is outside the steady state. Since we are working in the limit $\delta \to 0^+$, it will typically (in the strict sense) be the case that enough time has passed for the filtered state to have reached the steady state well before the next jump. Therefore, over the time before the second jump that we are interested in, the true state will be cyclically jumping between the three pure states in the PRE. Thus, the smoothed quantum state over this time range can be computed via

$$\rho_S(t) \propto \sum_{\theta\in\{\alpha,\beta,\phi\}} \mathrm{Tr}\left[\hat{E}_R(t)\rho(\theta)\right] \wp(\theta;t|\overleftarrow{\mathbf{O}}_t)\rho(\theta). \quad (41)$$

All that remains to compute the smoothed quantum state is to determine the probability distribution $\wp(\theta;t|\overleftarrow{\mathbf{O}}_t)$. This distribution is, by definition, the occupation probabilities of the PRE states, i.e., $\wp(\theta;t|\overleftarrow{\mathbf{O}}) = \wp_\theta$.

To check whether the smoothed quantum state is nondiagonal in the $\hat{\sigma}_z$ basis, we need to look at only the x component of its Bloch vector, as the y component is always zero for this adaptive local oscillator scheme. In Fig. 8, the x component (right-hand axis) and the length of the Bloch vector (left-hand axis), defined as $r = \sqrt{\langle\hat{\sigma}_x\rangle^2 + \langle\hat{\sigma}_y\rangle^2 + \langle\hat{\sigma}_z\rangle^2}$, for the smoothed quantum state are shown for this scheme (cyan). There are a couple of interesting features in this example, the most important being that the Bloch vector of the smoothed quantum state before the jump has nonzero x component. Thus, the smoothed quantum state is *not* diagonal in the $\hat{\sigma}_z$ basis, the shared basis of the filtered state and the retrofiltered effect, proving Result 2.

The reason the smoothed quantum state becomes nondiagonal is that Alice is able to infer from $\overrightarrow{\mathbf{O}}_t$, specifically the upcoming jump, that the two states in the PRE with a negative x component are more likely to have been occupied than they otherwise would be. This is because they have a larger overlap with the excited state than the single state with a positive x component. This breaks the symmetry of reflection around the z axis. This is evident in Fig. 9, where we can see the clear increase in the probability of the true state being in the PRE state on the far left and a substantial decrease in the probability of it being the PRE state closest to the ground state.

It should also be apparent, since the smoothed quantum state will be a mixture of the states in the PRE over the interval of interest, that the Bloch vector will lie within the triangle formed by the PRE states (the gray-shaded area in Fig. 7). As a result, the smoothed quantum state will not pass through the maximally mixed state (the center of the circle) as the observed jump approaches. This is not to say that the length of the Bloch vector does not decrease, it just does not go to zero. This can be seen in Fig. 8.

VIII. PROOF OF RESULT 3: COMPARING THE EXPECTED COST FUNCTIONS

As we have seen in the last two examples, the commutativity of the filtered state and the retrofiltered effect imposes no apparent constraints on the dynamics of the optimal smoothed quantum state. However, the fact that the optimal estimates in these cases are different gives rise to a new question. Alice cannot compute her optimal smoothed quantum state without knowledge of the nature of Bob's measurement, as this determines the set of possible true states. But what is the "best" measurement unraveling for Bob to perform from Alice's point of view? Since we already have a metric, the expected cost function, whose minimization defines the optimal estimate (ρ_F or ρ_S), it seems natural to use that expectation value as a measure of how good Alice's estimate is. For our particular cost function, this is equivalent to the measurement that results in the purest smoothed state.

Now, intuitively, the measurement for Bob that would give the greatest purity would be the measurement that causes $\rho_S(t) = \rho_S^{\mathrm{cl}}(t)$ as Alice only has to estimate between perfectly distinguishable true states. Applying this type of logic to the three cases that we have already considered, one would guess that after the case where Bob uses photon detection (having two perfectly distinguishable true states), the next best case would be the adaptive scheme (with three nonorthogonal true states), followed by the X homodyne case (with a continuous infinity of nonorthogonal states to distinguish). Comparing the expected cost functions for each estimate in Fig. 10, we can see that the above intuition is incorrect. The complete opposite holds for most of the time. This is despite the fact that the classically smoothed quantum state $\rho_S^{\mathrm{cl}}(t)$ is pure immediately before the jump occurs. We have already discussed how this is linked with a prior decrease in purity in the classical case; see Sec. V B. With only two states, with the steady state being relatively close to the ground state, and with the state just before the jump being the excited state, the classical smoothed state must pass through the maximally mixed state, at which point it must be the worst (highest expected cost) estimator. This leads us to Result 3, that the classically smoothed quantum state does not necessarily yield the lowest expected cost function.

We can gain more general intuition as to why increasing the number of possible true states yields purer smoothed estimates by analyzing the expression for the purity. That is,

$$P_S(t) = \mathrm{Tr}[\rho_S(t)^2] = \mathrm{Tr}\left[\left(\sum_{\rho_T\in\mathbb{T}_t} \wp(\rho_T; t|\overleftrightarrow{\mathbf{O}})\rho_T\right)^2\right]$$
$$= \sum_{\rho_T,\rho_T'\in\mathbb{T}_t} \wp(\rho_T; t|\overleftrightarrow{\mathbf{O}})\wp(\rho_T'; t|\overleftrightarrow{\mathbf{O}})\mathrm{Tr}[\rho_T\rho_T'], \quad (42)$$

where for ease of illustration we have assumed a discrete set of possible true states. We see that the purity is a weighted sum of the overlap between possible true states. Thus, with only two orthogonal true states in $\mathbb{T}_t$, the only terms that contribute are when $\rho_T = \rho_T'$. However, as the number of possible true states increases, additional terms that result from nonorthogonal states will also contribute, increasing the sum. Following this intuition, we arrive at the ordering that is observed in Fig. 10, over the great bulk of times. The exception is when the jump is imminent, where the ordering flips. (From Fig. 10, this flipping might appear to happen at an instant, but zooming in one finds that the three lines do not intersect at the same point in time.) In the photon detection case, the reason for the reversal is clear; as discussed above, just before Alice's jump, the state is pure and so the expected cost is zero. Something similar, but less dramatic, happens in the adaptive jump case. Just before Alice's jump, one of the three possible true states becomes much more likely than the others, as discussed in Sec. VII. We refer the reader to Fig. 9 again to appreciate the difference from the homodyne case.

As an aside, in Ref. [6] it was shown that the trace-square deviation from the true state is not the only cost function that has the smoothed state as its optimal estimator, so does the relative entropy. One might then ask whether the classically smoothed state gives the lowest expected relative entropy. The simple answer is "no"; the

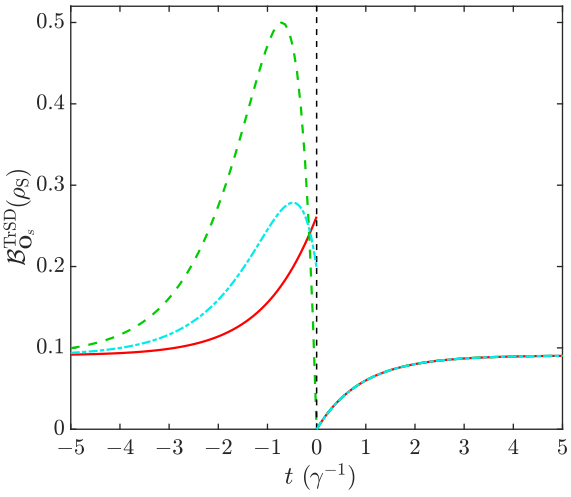

FIG. 10. Expected cost of the smoothed state when Alice's measurement record is obtained by photon detection and Bob's record is obtained by photon detection (dashed green line), an X homodyne measurement (red line), or an adaptive strategy based on weak local oscillators (dot-dashed cyan line); see Sec. VII. The expected cost for both the X homodyne case and the adaptive weak local oscillator case is lower than for the photon detection (classical) case most of the time due to the latter having to pass through the maximally mixed state to reach the (pure) excited state. See Fig. 5 for the parameter details. Time t has units of γ^{-1}.

ordering will not change. This is because, as shown in Ref. [6], when the true state is pure, the expected relative entropy between the smoothed state and the true state reduces to the von Neumann entropy. Since, for qubits, the von Neumann entropy is a monotonic function of the purity, the ordering will remain.

IX. CONCLUSION

To conclude this paper, let us revisit the question with which we opened it, in Fig. 1: Consider a two-level atom, undergoing incoherent excitation and radiative damping, with you monitoring some fraction of the output radiation. After some time, a photon is detected. What can we infer about the state of the atom immediately before emission of the photon?

We expected that most readers would intuitively answer "the excited state." As we showed in Sec. V B, this is exactly the answer given by classical smoothing theory, in which it is assumed that the true state of the atom is either the excited state or the ground state. However, as we have hopefully convinced the reader, this classical answer is not the "right" one, because there is a more general theory that can be applied—namely, quantum state smoothing. By considering a system that is isomorphic to this two-level atom with photon detection by observer Alice, we proved three results showing how the answer given by classical smoothing can be wrong.

Result 1 showed that the optimal smoothed estimate for this system in this situation depends on how the quantum information unobserved by Alice in the environment becomes classical. That is, to personify the process, it depends on how Bob measures the part of the environment Alice cannot access. For Result 1 we considered two different measurement schemes for Bob. When Bob's measurement scheme is, like Alice's, photon detection, this is equivalent to assuming a hidden Markov model comprising the ground and excited states, which are orthogonal. Then quantum state smoothing reduces to the classical theory and, immediately before Alice detects a photon, the smoothed quantum state is indeed the excited state. But if Bob performs homodyne detection, a different smoothed state is found. Immediately before Alice's detection, the smoothed quantum state is a classical mixture of the excited and ground states, and is weighted towards the latter. For the parameters we chose, it has a Jozsa fidelity [61] with the ground state of more than 84%.

While Result 1 proves that the answer given by applying classical smoothing is not necessarily correct, the smoothed quantum state calculated by Alice when Bob performs homodyne detection is still a mixture of the excited and ground states, just as in classical smoothing. Thus, it might be thought that it is just a worse version of classical smoothing. This thought is dispelled by Result 2. For this we considered a third type of measurement for Bob: an adaptive strategy using local oscillators and photon counters. Under this scheme, despite the apparent classicality of the system from Alice's perspective, the smoothed quantum state she calculates is not, in general, a classical mixture of ground and excited states. In particular, the smoothed state just before detection of a photon by her is much closer to the $\hat{\sigma}_x$ eigenstate $|-\rangle \propto |g\rangle - |e\rangle$, with a fidelity to that state greater than 87%.

Result 3 is the subtlest. In the face of Results 1 and 2, one might still hope that the classical smoothing technique would be better than the other techniques; that the simplicity of the photon detection scheme for Bob, relative to the others (homodyne and adaptive), would be reflected in Alice's ability to estimate the resulting unknown record and hence estimate the associated true state. (This ability is quantified by the trace-squared deviation between the true state and the state estimate, which is the cost function whose minimization defines the optimal estimate.) Contrary to this intuition, we showed in our example that, most of the time, the expected cost is *higher* for the classical smoothing technique than for the quantum smoothing technique appropriate for the other unravelings.

What are the implications of our work for experiments estimating a quantum state using past and future information, especially those experiments [2–5] in which classical smoothing theory was applied? In the first place, Results 1 and 2 show the importance of stating exactly what assumptions one is making about the underlying true dynamics of the system if one applies any given quantum state smoothing technique. In particular, even when it seems one can apply an effectively classical smoothing theory, because Alice's filtering and retrofiltering can be described classically in a fixed basis, one must assume that the true state of the system has no coherences in that basis. Furthermore, Result 3 shows that, given one must make an assumption on the true state dynamics, one can get an even better estimate of the assumed true state by considering nonclassical dynamics. That is, if one restricts oneself to classical state smoothing, then one's estimate may be further from the assumed true states on average.

The reader might be wondering whether the use of classical smoothing in Refs. [2–5] could be justified by an argument based on decoherence [43,44] (although we note that no such argument was made explicitly in those papers). Such an argument would have to claim that if the dynamics, including Alice's information gathering, can be described diagonally in a fixed basis, then decoherence acting at the level of the system causes an effective collapse into one of the diagonal states. However, while decoherence may lead to effective collapse for large many-body quantum systems [43,44], there is no good reason for applying it to microscopic quantum systems. Indeed, as we showed, it is easy to imagine realistic measurement schemes performed by Bob that rely on the existence of entanglement between the system and its environment.

It is only at the level of the macroscopic measuring instruments (both Alice's and Bob's) that it is safe to invoke decoherence and collapse.

The clearest way to refute the decoherence argument mooted above would be to experimentally verify the predictions of this paper. This would involve implementing the measurement by Alice and the various measurements by Bob, and verifying the optimality (in terms of the cost function used) of Alice's smoothed estimate of the filtered state Bob computes. (The reliability of the latter would first have to be verified independently.) The example system we considered would, however, be quite challenging at the current stage of quantum technology. Physically implementing Bob's measurement would mean that we would have to be able to detect the vast majority of the emitted light with high-efficiency detectors to ensure a near-pure "true state." Additionally, to implement the adaptive scheme in Sec. VII would require fast light modulation (compared with the atomic transition rates), which is challenging given typical electrical and the electro-optic response times.

However, there are reasons to be optimistic that the central results in this paper would be considerably easier to demonstrate than the discussion above suggests. First, the system we considered is only one way to prove the results. Second, even with use of the same system, it would not be necessary to realize the conditioned dynamics perfectly. In particular, one does not require Bob's filtered state (the "true state") to be pure. With use of a cavity QED setup, a reasonably large measurement efficiency should be possible for direct and homodyne detection, which would suffice to show Results 1 and 3. Third, there may well be a nonadaptive scheme that could demonstrate Result 2, thereby avoiding fast modulation. An alternative route to experimental tests is to discretize the open quantum system dynamics in time, so that one could simulate the system we have proposed, or something similar to it, on a quantum computer. Here the bath interactions would be modeled by successive gates on an array of qubits, i.e., a collision model [62]. The details of this proposal are left for future work.

Our results raise several other theoretical research questions. While we have shown that a classical description of Alice's filtering and retrofiltering is not sufficient for classical smoothing to be applicable in general, and that a classical description of the true state *is* sufficient, we do not know whether the latter condition is necessary, or whether some weaker condition would be sufficient. Another question is whether, given a classical description of Alice's filtering and retrofiltering, there could be a different cost function such that the classically smoothed quantum state in Eq. (11) would be the optimal estimator for quantum systems. Outside this regime, another way that one might try to apply classical smoothing would be to diagonalize the filtered state at each instant in time and then compute new weightings for those eigenstates using classical smoothing. Lastly, as mentioned in Ref. [46], it would be interesting to investigate what would happen if Alice assumed that Bob's unraveling had a classical description when in fact it does not. How poorly does this "wrongly guessed" smoothed state perform in terms of the trace-square deviation, and could we find unravelings for Bob (or even Alice) that minimize the deviation from the optimal expected cost?

ACKNOWLEDGMENTS

This research was funded by the Australian Research Council Centre of Excellence Program, Grant No. CE170100012. K.T.L. was supported by an Australian Government Research Training Program Scholarship. A.C. acknowledges the support of the NSRF of Thailand via the Program Management Unit for Human Resources & Institutional Development, Research and Innovation, Grant No. B05F650024.

APPENDIX A: CO-DIAGONALITY OF THE FILTERED STATE AND THE RETROFILTERED EFFECT

In this appendix we prove that when $\rho_T(t) \in \mathbb{T}_{\text{diag}} = \{|\psi_m\rangle\langle\psi_m| : \langle\psi_m|\psi_{m'}\rangle = \delta_{m,m'}\}$, both the filtered state (provided the state is initially diagonal in this basis) and the retrofiltered effect are necessarily diagonal in any basis that contains these states. However, before we present the proof, we need to express how both the true state and filtered quantum state evolve in terms of quantum maps. For the true quantum state, a measurement operator [15,16] is assigned for each measurement outcome, which we denote as $\hat{M}_o(\mathbf{y}_o; t)$, where $\mathbf{y}_o(t)$ denotes the observed measurement outcome, and similarly for the unobserved measurement, be it a detector click or a photocurrent. With these measurement operators, the true state evolves as follows [47]:

$$\tilde{\rho}_T(t+dt) = \hat{M}_o(\mathbf{y}_o; t)\hat{M}_u(\mathbf{y}_u; t)\tilde{\rho}_T(t)\hat{M}_u^\dagger(\mathbf{y}_u; t)\hat{M}_o^\dagger(\mathbf{y}_o; t). \tag{A1}$$

Here, for a later derivation, we have refrained from normalizing the state at each time step, as indicated by the tilde. Note that for notational simplicity we have absorbed the operator that generates the deterministic part of the evolution (including the Hamiltonian part of the evolution) into the observed measurement operator.

For the filtered quantum state, conditioning is done only on the observed measurement record, with the unobserved channel contributing the decoherence affecting the state. In general, one can recover the appropriate dynamics of the filtered state by averaging over the possible unobserved records. Averaging Eq. (A1) over the unobserved measurement record, we find the (unnormalized) filtered state

evolves according

$$\tilde{\rho}_F(t+dt) = \sum_{\mathbf{y}_u(t)} \hat{M}_o(\mathbf{y}_o;t)\hat{M}_u(\mathbf{y}_u;t)\tilde{\rho}_F(t)\hat{M}_u^\dagger \times (\mathbf{y}_u;t)\hat{M}_o^\dagger(\mathbf{y}_o;t), \tag{A2}$$

where we have assumed, for simplicity, that the spectrum of measurement outcomes is discrete. For a continuous spectrum, this sum is replaced by an appropriate integral. To determine how the retrofiltered effect evolves, we use the fact that $\mathrm{Tr}[\tilde{\rho}_F(t)\hat{E}_R(t)] = \tilde{\wp}(\overleftrightarrow{\mathbf{O}})$, which is independent of the time t. Thus, we have $\mathrm{Tr}[\tilde{\rho}_F(t)\hat{E}_R(t)] = \mathrm{Tr}[\tilde{\rho}_F(t+dt)\hat{E}_R(t+dt)]$. Applying Eq. (A2), the cyclic property of the trace, and the fact that this holds for all possible filtered states gives us the dynamical equation for the retrofiltered effect:

$$\hat{E}_R(t) = \sum_{\mathbf{y}_u(t)} \hat{M}_u^\dagger(\mathbf{y}_u;t)\hat{M}_o^\dagger(\mathbf{y}_u;t)\hat{E}_R(t+dt) \times \hat{M}_o(\mathbf{y}_o;t)\hat{M}_u(\mathbf{y}_u;t). \tag{A3}$$

Proof.—Given that $\rho_T(t) \in \mathbb{T}_{\mathrm{diag}}$ over the interval $[t_i, t_f)$, Eq. (A1) becomes

$$|\psi_i\rangle\langle\psi_i| \propto \hat{M}_o(\mathbf{y}_o;t)\hat{M}_u(\mathbf{y}_u;t)|\psi_j\rangle\langle\psi_j|\hat{M}_u^\dagger(\mathbf{y}_u;t)\hat{M}_o^\dagger(\mathbf{y}_o;t). \tag{A4}$$

By expressing the product of measurement operators as $\hat{M}_o(\mathbf{y}_o;t)\hat{M}_u(\mathbf{y}_u;t) = \sum_{i,j} T_{i,j}(\mathbf{y}_u;t)|\psi_i\rangle\langle\psi_j|$, Eq. (A4) places a restriction on the matrix elements $T_{i,j}(\mathbf{y}_u;t)$. Specifically, we have $T_{i,k}(\mathbf{y}_u;t)T^*_{k,j}(\mathbf{y}_u;t) \propto \delta_{i,j}$, where A^* denotes the complex conjugate of A. Note that since we are averaging over only the unobserved measurement, we have dropped the dependence on $\mathbf{y}_o(t)$ in the matrix elements for notational simplicity. Importantly, this constraint holds for all possible realizations of $\mathbf{y}_u(t)$ since the set $\mathbb{T}_{\mathrm{diag}}$ contains the possible true states for any realization of $\overleftarrow{\mathbf{O}}_t$ and $\overleftarrow{\mathbf{U}}_t$.

With this constraint on the measurement operators, we can now compute the filtered state. Beginning with Eq. (A2), we have

$$\tilde{\rho}_F(t+dt) = \sum_{\mathbf{y}_u(t)}\sum_{i,j,k,\ell} T_{ij}(\mathbf{y}_u;t)T^*_{k\ell}(\mathbf{y}_u;t) \times |\psi_i\rangle\langle\psi_j|\tilde{\rho}_F(t)|\psi_k\rangle\langle\psi_\ell|. \tag{A5}$$

Assuming that the filtered state is diagonal at time t, i.e., $\tilde{\rho}_F(t) = \sum_m \tilde{\wp}_F(m;t)|\psi_m\rangle\langle\psi_m|$, we have

$$\tilde{\rho}_F(t+dt) = \sum_{\mathbf{y}_u(t)}\sum_{i,j,k,\ell,m} T_{ij}(\mathbf{y}_u;t)T^*_{k\ell}(\mathbf{y}_u;t)\tilde{\wp}_F(m;t) \times |\psi_i\rangle\langle\psi_j|\psi_m\rangle\langle\psi_m|\psi_k\rangle\langle\psi_\ell| \tag{A6}$$

$$= \sum_{\mathbf{y}_u(t)}\sum_{i,j,k,\ell,m} T_{ij}(\mathbf{y}_u;t)T^*_{k\ell}(\mathbf{y}_u;t)\tilde{\wp}_F(m;t)\delta_{j,m}\delta_{m,k}|\psi_i\rangle\langle\psi_\ell| \tag{A7}$$

$$= \sum_{\mathbf{y}_u(t)}\sum_{i,j,\ell} T_{ij}(\mathbf{y}_u;t)T^*_{j\ell}(\mathbf{y}_u;t)\tilde{\wp}_F(j;t)|\psi_i\rangle\langle\psi_\ell| \tag{A8}$$

$$= \sum_{\mathbf{y}_u(t)}\sum_{i,j,\ell} c_i(\mathbf{y}_u;t)\tilde{\wp}_F(j;t)\delta_{i,\ell}|\psi_i\rangle\langle\psi_\ell| \tag{A9}$$

$$= \sum_{\mathbf{y}_u(t)}\sum_{i,j} c_i(\mathbf{y}_u;t)\tilde{\wp}_F(j;t)|\psi_i\rangle\langle\psi_i|, \tag{A10}$$

where, in Eq. (A9), we have substituted the condition $T_{i,j}(\mathbf{y}_u;t)T^*_{j,\ell}(\mathbf{y}_u;t) = c_i(\mathbf{y}_u;t)\delta_{i,\ell}$, where $c_i(\mathbf{y}_u;t) \in \mathbb{R}$ is the constant of proportionality. Importantly, we see that the quantum maps that generate the evolution of the filtered state preserve the diagonality in the orthogonal basis $\{|\psi_m\rangle\}_m$. Thus, provided the initial condition is diagonal in the basis $\{|\psi_m\rangle\}_m$, the filtered state will remain diagonal while $\rho_T \in \mathbb{T}_{\mathrm{diag}}$.

For the retrofiltered effect, the proof follows in a manner similar to that for the filtered state. Beginning by substituting the measurement operator into Eq. (A3) and assuming the retrofiltered effect at t is diagonal in this basis, i.e., $\hat{E}_R(t+dt) = \sum_m E_R(m;t+dt)|\psi_m\rangle\langle\psi_m|$, we have

$$\hat{E}_R(t) = \sum_{\mathbf{y}_u(t)}\sum_{i,j,k,\ell,m} T^*_{ij}(\mathbf{y}_u;t)T_{k\ell}(\mathbf{y}_u;t)E_R(m;t+dt) \times |\psi_i\rangle\langle\psi_j|\psi_m\rangle\langle\psi_m|\psi_k\rangle\langle\psi_\ell| \tag{A11}$$

$$= \sum_{\mathbf{y}_u(t)}\sum_{i,j,\ell} T^*_{ij}(\mathbf{y}_u;t)T_{j\ell}(\mathbf{y}_u;t)E_R(j;t+dt)|\psi_i\rangle\langle\psi_\ell| \tag{A12}$$

$$= \sum_{\mathbf{y}_u(t)}\sum_{i,j,\ell} c_i(\mathbf{y}_u;t)E_R(j;t+dt)\delta_{i,\ell}|\psi_i\rangle\langle\psi_\ell| \tag{A13}$$

$$= \sum_{\mathbf{y}_u(t)}\sum_{i,j} c_i(\mathbf{y}_u;t)E_R(j;t+dt)|\psi_i\rangle\langle\psi_i|, \tag{A14}$$

where in Eq. (A13) we have used the fact that $T^*_{ij}(\mathbf{y}_u;t)T_{j\ell}(\mathbf{y}_u;t) = (T_{ij}(\mathbf{y}_u;t)\,T^*_{j\ell}(\mathbf{y}_u;t))^* = c_i(\mathbf{y}_u;t)\delta_{i,\ell}$. Once again, we see that the quantum maps that generate the evolution of the retrofiltered effect preserve the diagonality in the orthogonal basis $\{|\psi_i\rangle\}_i$. Thus, since $\hat{E}_R(t_f) \propto \hat{1}$, which is diagonal in every basis, the retrofiltered effect is necessarily diagonal when $\rho_T \in \mathbb{T}_{\mathrm{diag}}$. ■

APPENDIX B: SPECIFICATION OF THE ADAPTIVE MEASUREMENT SCHEME

In this paper the physical system of interest is a qubit coupled to three decoherence channels: two emission channels (one monitored by Alice and one monitored by Bob) and one absorption channel (monitored by Bob). In Sec.

VII, the emission channel monitored by Alice is assumed to be very weak, $\delta \to 0^+$, meaning that in the long periods between her observed detections, her filtered state will reach a steady state. In some parameter regimes [57] it is then possible for Bob to restrict the system state to a finite and time-independent set $\mathbb{T}$, which is known as a PRE. For this to occur, Bob must use a carefully chosen adaptive measurement scheme to monitor his emission and absorption channels. In Sec. VII, Bob is assumed to enact such a measurement scheme, which leads to the PRE in Fig. 7 when $\epsilon = 0.05\gamma$. The PRE in question consists of three states (α, β, and ϕ) that are labeled by the angle of the Bloch vector in the x-z great circle of the Bloch sphere.

The freedom that Bob has when choosing his measurement scheme is most easily understood in a quantum optics context. Bob may use linear interferometers that take the field outputs of the system as inputs. He may also use weak local oscillators (WLOs) that can be added to the interferometer outputs before photon detection. To achieve the PRE in Sec. VII, it turns out that Bob can use a relatively simple measurement scheme that uses only WLOs and does *not* mix the system outputs. The measurement scheme is further simplified as it obeys symmetries present in the unconditional evolution—namely, that real-valued density matrices remain real valued under the action of $\mathcal{L} = \mathcal{D}[\hat{\mathbf{c}}]$. Thus, Bob separately adds a real-valued WLO to his emission and absorption channels before photon detection. The scheme is adaptive in the sense that the WLO amplitudes must be varied according to which state of the PRE is occupied.

Before specifying the constraint equations that define the measurement scheme, we define the effective no-jump Hamiltonian, $\hat{H}'_{\text{eff}}$, and jump operators, $\hat{\sigma}'_{\mp}$, that are applicable when Bob is using real-valued WLOs. The non-Hermitian operator $\hat{H}'_{\text{eff}}$ defines Bob's filtered system evolution in time increments when he observes no detections, whereas $\hat{\sigma}'_{\mp}$ is proportional to the measurement operator used by Bob to evolve the state upon a detection from either of the two channels that he is monitoring. For example, if the system state is currently $|\alpha\rangle$, then

$$\hat{H}'_{\text{eff}}(\alpha) = -\frac{i}{2}\Big(\gamma\hat{\sigma}_-^\dagger\hat{\sigma}_- + \epsilon\hat{\sigma}_+^\dagger\hat{\sigma}_+ \times +2\sqrt{\gamma}\alpha_-\hat{\sigma}_- + 2\sqrt{\epsilon}\alpha_+\hat{\sigma}_+ + \alpha_-^2 + \alpha_+^2\Big), \tag{B1}$$

$$\hat{\sigma}'_-(\alpha) = \hat{\sigma}_- + \alpha_-, \tag{B2}$$

$$\hat{\sigma}'_+(\alpha) = \hat{\sigma}_+ + \alpha_+, \tag{B3}$$

where α_- and α_+ are the WLO amplitudes added to the emission and absorption channels, respectively. The jump and no-jump operators for the other states of the PRE are obtained simply by changing the WLO amplitudes to $\phi_{\mp}$ and $\beta_{\mp}$. The values of all of these WLO amplitudes are yet to be determined.

The cyclic PRE is then defined by requiring that each of the PRE states is an eigenstate of the appropriate no-jump operator,

$$\hat{H}'_{\text{eff}}(\alpha)|\alpha\rangle \propto |\alpha\rangle, \tag{B4}$$

$$\hat{H}'_{\text{eff}}(\phi)|\phi\rangle \propto |\phi\rangle, \tag{B5}$$

$$\hat{H}'_{\text{eff}}(\beta)|\beta\rangle \propto |\beta\rangle, \tag{B6}$$

and that the jump operators cyclically move the state around the ensemble:

$$\hat{\sigma}'_-(\alpha)|\alpha\rangle \propto |\phi\rangle, \quad \hat{\sigma}'_+(\alpha)|\alpha\rangle \propto |\phi\rangle, \tag{B7}$$

$$\hat{\sigma}'_-(\phi)|\phi\rangle \propto |\beta\rangle, \quad \hat{\sigma}'_+(\phi)|\phi\rangle \propto |\beta\rangle, \tag{B8}$$

$$\hat{\sigma}'_-(\beta)|\beta\rangle \propto |\alpha\rangle, \quad \hat{\sigma}'_+(\beta)|\beta\rangle \propto |\alpha\rangle. \tag{B9}$$

Given that the states comprising the PRE are known, Eqs. (B4)–(B9) can be easily solved numerically for $\alpha_{\mp}$, $\phi_{\mp}$, and $\beta_{\mp}$. It is worth noting that rounding errors in the specification of the PRE states mean that a minimization approach to solving the constraints is necessary (such as minimizing the sum of the constraints squared). Also important is that we have not specified how the PRE states are found in the first place; rather we have focused on the appropriate measurement scheme to achieve the PRE. Techniques for finding the PRE are discussed elsewhere [57], but here we actually apply it to derive the measurement scheme. The values we find for $\alpha_{\mp}$, $\phi_{\mp}$, and $\beta_{\mp}$ are as follows (with the upper and lower values matching the $-$ and $+$ subscripts):

$$\alpha_{\mp} = \begin{bmatrix} -0.07812 \\ -0.1804 \end{bmatrix}, \quad \phi_{\mp} = \begin{bmatrix} -0.3684 \\ 0.2552 \end{bmatrix}, \quad \beta_{\mp} = \begin{bmatrix} 0.06446 \\ 0.6158 \end{bmatrix}. \tag{B10}$$

As an example, when Bob knows the system state is $|\phi\rangle$, he should add a WLO of amplitude -0.3684 to the emission channel and a WLO of amplitude 0.2552 to the absorption channel. If he does this, then the system will stay in the state $|\phi\rangle$ until he registers a detection. Upon registering a detection (from either of his photon detectors) the system state will jump to $|\beta\rangle$. Bob then should immediately switch the WLO amplitudes to $\beta_{\mp}$, which will stabilize the system in state $|\beta\rangle$. In this way, Bob will know the system state and restrict it to the PRE $\mathbb{T}$. As a final point, more than one measurement scheme capable of realizing the PRE in Fig. 7 was discovered in our investigation, with the scheme in Eq. (B10) possessing the most symmetry. This measurement scheme freedom may be explored further elsewhere.

[1] I. Guevara and H. M. Wiseman, Quantum state smoothing, Phys. Rev. Lett. **115**, 180407 (2015).

[2] M. A. Armen, A. E. Miller, and H. Mabuchi, Spontaneous dressed-state polarization in the strong driving regime of cavity QED, Phys. Rev. Lett. **103**, 173601 (2009).

[3] J. Kerckhoff, M. A. Armen, D. S. Pavlichin, and H. Mabuchi, The dressed atom as binary phase modulator: Towards attojoule/edge optical phase-shift keying, Opt. Exp. **19**, 6478 (2011).

[4] S. Gammelmark, K. Mølmer, W. Alt, T. Kampschulte, and D. Meschede, Hidden Markov model of atomic quantum jump dynamics in an optically probed cavity, Phys. Rev. A **89**, 043839 (2014).

[5] T. Rybarczyk, B. Peaudecerf, M. Penasa, S. Gerlich, B. Julsgaard, K. Mølmer, S. Gleyzes, M. Brune, J. M. Raimond, and S. Haroche, *et al.*, Forward-backward analysis of the photon-number evolution in a cavity, Phys. Rev. A **91**, 062116 (2015).

[6] K. T. Laverick, I. Guevara, and H. M. Wiseman, Quantum state smoothing as an optimal Bayesian estimation problem with three different cost functions, Phys. Rev. A **104**, 032213 (2021).

[7] A. Chantasri, I. Guevara, K. T. Laverick, and H. M. Wiseman, Unifying theory of quantum state estimation using past and future information, Phys. Rep. **930**, 1 (2021).

[8] C. Robert, *The Bayesian Choice: From Decision-Theoretic Foundations to Computational Implementation* (Springer Science & Business Media, New York, 2007).

[9] F. J. Samaniego, *A Comparison of the Bayesian and Frequentist Approaches to Estimation* (Springer Science & Business Media, New York, 2010).

[10] G. Parmigiani and L. Inoue, *Decision Theory: Principles and Approaches* (Wiley, Chichester, 2009), Vol. 812.

[11] J. O. Berger, *Statistical Decision Theory and Bayesian Analysis* (Springer Science & Business Media, New York, 2013).

[12] V. P. Belavkin, in *Information, Complexity and Control in Quantum Physics*, edited by A. Blaquíere, S. Dinar, and G. Lochak (Springer, New York, 1987).

[13] V. P. Belavkin, Quantum continual measurements and a posteriori collapse on CCR, Commun. Math. Phys. **146**, 611 (1992).

[14] H. J. Carmichael, *An Open Systems Approach to Quantum Optics* (Springer, Berlin, 1993).

[15] H. M. Wiseman and G. J. Milburn, *Quantum Measurement and Control* (Cambridge University Press, Cambridge, England, 2010).

[16] H.-P Breuer and F. Petruccione, *The Theory of Open Quantum Systems* (Oxford University Press, New York, 2006).

[17] A. Barchielli and M. Gregoratti, *Quantum Trajectories and Measurements in Continuous Time* (Springer, New York, 2009).

[18] M. Tsang, Optimal waveform estimation for classical and quantum systems via time-symmetric smoothing, Phys. Rev. A **80**, 033840 (2009).

[19] M. Tsang, Optimal waveform estimation for classical and quantum systems via time-symmetric smoothing. II. Applications to atomic magnetometry and Hardy's paradox, Phys. Rev. A **81**, 013824 (2010).

[20] K. Ohki, in *Proceedings of the ISCIE International Symposium on Stochastic Systems Theory and Its Applications* (Tokyo, Japan, 2022), p. 8.

[21] H. Mabuchi and A. C. Doherty, Cavity quantum electrodynamics: Coherence in context, Science **298**, 1372 (2002).

[22] H. Mabuchi and H. M. Wiseman, Retroactive quantum jumps in a strongly coupled atom-field system, Phys. Rev. Lett. **81**, 4620 (1998).

[23] C. Benedetti, F. Buscemi, P. Bordone, and M. G. A. Paris, Quantum probes for the spectral properties of a classical environment, Phys. Rev. A **89**, 032114 (2014).

[24] E. Kleinherbers, P. Stegmann, A. Kurzmann, M. Geller, A. Lorke, and J. König, Pushing the limits in real-time measurements of quantum dynamics, Phys. Rev. Lett. **128**, 087701 (2022).

[25] M. Tsang, Time-symmetric quantum theory of smoothing, Phys. Rev. Lett. **102**, 250403 (2009).

[26] M. Tsang, J. H. Shapiro, and S. Lloyd, Quantum theory of optical temporal phase and instantaneous frequency. II. Continuous-time limit and state-variable approach to phase-locked loop design, Phys. Rev. A **79**, 053843 (2009).

[27] H. Yonezawa, D. Nakane, T. A. Wheatley, K. Iwasawa, S. Takeda, H. Arao, K. Ohki, K. Tsumura, D. W. Berry, and T. C. Ralph, *et al.*, Quantum-enhanced optical-phase tracking, Science **337**, 1514 (2012).

[28] K. Iwasawa, K. Makino, H. Yonezawa, M. Tsang, A. Davidovic, E. Huntington, and A. Furusawa, Quantum-limited mirror-motion estimation, Phys. Rev. Lett. **111**, 163602 (2013).

[29] T. A. Wheatley, M. Tsang, I. R. Petersen, and E. H. Huntington, Improved mirror position estimation using resonant quantum smoothing, EPJ Quantum Technol. **2**, 1 (2015).

[30] S. Roy, I. R. Petersen, and E. H. Huntington, Robust adaptive quantum phase estimation, New J. Phys. **17**, 063020 (2015).

[31] Z. Huang and M. Sarovar, Smoothing of Gaussian quantum dynamics for force detection, Phys. Rev. A **97**, 042106 (2018).

[32] C. Zhang and K. Mølmer, Estimating a fluctuating magnetic field with a continuously monitored atomic ensemble, Phys. Rev. A **102**, 063716 (2020).

[33] S. Gammelmark, B. Julsgaard, and K. Mølmer, Past quantum states of a monitored system, Phys. Rev. Lett. **111**, 160401 (2013).

[34] D. Tan, M. Naghiloo, K. Mølmer, and K. W. Murch, Quantum smoothing for classical mixtures, Phys. Rev. A **94**, 050102(R) (2016).

[35] H. Bao, J. Duan, S. Jin, X. Lu, P. Li, W. Qu, M. Wang, I. Novikova, E. E. Mikhailov, and K. F. Zhao, *et al.*, Spin squeezing of 10^{11} atoms by prediction and retrodiction measurements, Nature **581**, 159 (2020).

[36] K. Ohki, in *54th IEEE Conference on Decision and Control (CDC)* (IEEE, Osaka, Japan, 2015), p. 4350.

[37] K. Ohki, in *Proceedings of the ISCIE International Symposium on Stochastic Systems Theory and Its Applications* (Fukushima, Japan, 2019), p. 25.

[38] M. Tsang, Generalized conditional expectations for quantum retrodiction and smoothing, Phys. Rev. A **105**, 042213 (2022).

[39] A. A. Budini, Smoothed quantum-classical states in time-irreversible hybrid dynamics, Phys. Rev. A **96**, 032118 (2017).

[40] A. A. Budini, Quantum non-Markovian processes break conditional past-future independence, Phys. Rev. Lett. **121**, 240401 (2018).

[41] K. T. Laverick, A. Chantasri, and H. M. Wiseman, General criteria for quantum state smoothing with necessary and sufficient criteria for linear Gaussian quantum systems, Quantum Stud. Math. Found. **8**, 37 (2021).

[42] While we consider the case where the environment unravels the remaining $1-\eta$ fraction, it is not necessary for the theory but rather stems from the context we are applying the smoothing theory to. In the scenario where there are two real observers, Alice and Bob, one can replace this fraction by Bob's measurement efficiency η_u, where Alice's efficiency and Bob's efficiency may not sum to unity.

[43] W. H. Zurek, Decoherence, einselection, and the quantum origins of the classical, Rev. Mod. Phys. **75**, 715 (2003).

[44] P. Strasberg, Classicality with(out) decoherence: Concepts relation to Markovianity, and a random matrix theory approach, SciPost Phys. **15**, 024 (2023).

[45] K. T. Laverick, A. Chantasri, and H. M. Wiseman, Quantum state smoothing for linear Gaussian systems, Phys. Rev. Lett. **122**, 190402 (2019).

[46] A. Chantasri, I. Guevara, and H. M. Wiseman, Quantum state smoothing why the types of observed and unobserved measurements matter, New J. Phys. **21**, 083039 (2019).

[47] I. Guevara and H. M. Wiseman, Completely positive quantum trajectories with applications to quantum state smoothing, Phys. Rev. A **102**, 052217 (2020).

[48] A. Kuhn, M. Hennrich, and G. Rempe, Deterministic single-photon source for distributed quantum networking, Phys. Rev. Lett. **89**, 067901 (2002).

[49] A. B. Klimov, J. L. Romero, J. Delgado, and L. L. Sánchez-Soto, Effective damping in the Raman cooling of trapped ions, Opt. Commun. **230**, 393 (2004).

[50] M. Keller, B. Lange, K. Hayasaka, W. Lange, and H. Walther, Continuous generation of single photons with controlled waveform in an ion-trap cavity system, Nature **431**, 1075 (2004).

[51] S. Sun, J. L. Zhang, K. A. Fischer, M. J. Burek, C. Dory, K. G. Lagoudakis, Y.-K. Tzeng, M. Radulaski, Y. Kelaita, and A. Safavi-Naeini, *et al.*, Cavity-enhanced Raman emission from a single color center in a solid, Phys. Rev. Lett. **121**, 083601 (2018).

[52] C. W. Gardiner, *Handbook of Stochastic Methods for Physics, Chemistry and the Natural Sciences* (Springer, Berlin, 2004).

[53] J. Gambetta and H. M. Wiseman, Stochastic simulations of conditional states of partially observed systems, quantum and classical, J. Opt. B: Quantum Semiclass. Opt. **7**, S250 (2005).

[54] S. J. Dolinar, An optimum receiver for the binary coherent state quantum channel, MIT Res. Lab. Electron. Q. Prog. Rep. **111**, 115 (1973).

[55] C. W. Helstrom, *Quantum Detection and Estimation Theory*. Mathematics in Science and Engineering, Vol. 123 (Academic Press, New York, 1976).

[56] S. Daryanoosh and H. M. Wiseman, Quantum jumps are more quantum than quantum diffusion, New J. Phys. **16**, 063028 (2014).

[57] P. Warszawski and H. M. Wiseman, Symmetries and physically realisable ensembles for open quantum systems, New J. Phys. **21**, 053006 (2019).

[58] P. Warszawski and H. M. Wiseman, Open quantum systems are harder to track than open classical systems, Quantum **3**, 192 (2019).

[59] H. M. Wiseman and J. A. Vaccaro, Inequivalence of pure state ensembles for open quantum systems: The preferred ensembles are those that are physically realizable, Phys. Rev. Lett. **87**, 240402 (2001).

[60] L. Li, M. J. W. Hall, and H. M. Wiseman, Concepts of quantum non-Markovianity: A hierarchy, Phys. Rep. **759**, 1 (2018).

[61] R. Jozsa, Fidelity for mixed quantum states, J. Mod. Opt. **41**, 2315 (1994).

[62] M. Cattaneo, G. De Chiara, S. Maniscalco, R. Zambrini, and G. L. Giorgi, Collision models can efficiently simulate any multipartite Markovian quantum dynamics, Phys. Rev. Lett. **126**, 130403 (2021).